PUSH-IT

Piloting Underground Seasonal Heat Storage In geothermal reservoirs

D3.3 Evaluation of Co-Simulation results lessons learned for application and optimization

Funded by the European Union

Grant agreement number	101096566		
Project title	Piloting Underground Storage of Heat In geoThermal reservoirs		
Project acronym	PUSH-IT		
Start date	01-01-2023	DURATION	48 months
End date	31-12-2026		
Work Package No. and Title	WP3 Enabling technologies		
Deliverable number	D3.3		
Deliverable title	Evaluation of Co-Simulation results lessons learned for application and optimisation		
Actual date of delivery	20-07-2026		
Nature	R	DISSEMINATION LEVEL	Public
Deliverable Leader	TDA		
Author	M. Ohagen		
Co-authors and contributors	H. Pham, E. Kukrer, T. Spengler, W. Hagemann, M. Krusemark, M. Schedel		

Disclaimer

Funded by the European Union

Funded by the European Union under the Horizon Europe programme (grant no. 1011096566). Views and opinions expressed are however those of the author(s) only and do not necessarily reflect those of the European Union. Neither the European Union nor CINEA can be held responsible for them.

Document history

Version	Description (Section, page number)	Author	Role (Organisation short name)
V0.1	First draft	Max Ohagen, Hung Pham, Ergin Kükrer, Till Spengler Willem Hagemann, Matthias Krusemark, Markus Schedel	TDA, TUD, F-IEG
V0.2	Second draft Processed of feedback received from reviewers / partners	Max Ohagen	TDA
V0.3	Draft final Processed of feedback received from reviewers / partners	Max Ohagen	TDA
V1.0	Final version	Max Ohagen	TUD

Quality control

Author	Organisation short name	Role	Date
Phil Vardon	TUD	Work Package Leader	09-07-2026
Max Ohagen	TDA	Deliverable Leader	06-07-2026
Dirk Vanhoudt	VITO	Reviewer 1	23-06-2026
Ergin Kukrer	TUD	Reviewer 2	28-06-2026
Martin Bloemendal	TUD	Scientific Project Coordinator	20-07-2026
Danitsja van Heusden	TUD	Project Coordinator	20-07-2026

Executive Summary

This Deliverable (D3.3) reports the co-simulation work carried out within Task 3.4.2 of Work Package 3 and evaluates its results across the three PUSH-IT demonstration sites. Co-simulation, as applied here, couples a domain-specific subsurface storage model to a surface-side energy system model. Each component simulator runs in its native environment and boundary conditions, while exchanging simulation parameters at defined synchronization points at runtime. This preserves the numerical fidelity of both domains and captures the dynamic feedback between the evolving subsurface temperature field and surface-side operation, dynamics that standalone simulations cannot reproduce. The approach was applied to three storage technologies and geological settings: borehole thermal energy storage (BTES) at Darmstadt, aquifer thermal energy storage (ATES) at Delft, and mine thermal energy storage (MTES) at Bochum.

Two coupling mechanisms were used successfully: direct Python APIs (FEFLOW via the IFM interface, OpenDARTS, and the Python MTES model) and the Functional Mock-up Interface (FMI), through which Modelica energy-system models were exported as FMUs and driven from a Python orchestration layer. The choice between them was governed by the tools involved rather than any inherent advantage.

At Darmstadt, a FEFLOW model of three 750 m deviated borehole heat exchangers was coupled to a Modelica surface model to diagnose the site's persistent discharge limitation. The simulations identify the hydraulic connection point as the decisive factor: connecting the BTES downstream of an individual building substation yields recovery efficiencies below 1.1 %, whereas relocating it to the aggregated central return pipe raises the fifth-year efficiency to 20.9 %. An upscaled 37-BHE configuration with a 4 MW heat pump reaches 74.8 %, demonstrating that field size, not the storage concept, constrains the current installation.

At Delft, a DARTS reservoir model was coupled to a TESPy surface model over a ten-year horizon. The ATES wells warm up gradually over roughly six years. Early on, part of the geothermal supply is used to heat the initially cold storage. As the wells heat up, the share going to charging falls from 45.5 % to 34.5 %, discharge becomes more consistent, CHP/boiler use drops, and the renewable share exceeds 95 % by year ten. A dynamic cut-off control further improves operation as the aquifer heats up.

At Bochum, a low-order, physics-based Python MTES model was coupled to a Modelica surface model via an FMU. The system behaves as a seasonal storage, with the surrounding rock reaching quasi-steady equilibrium after about three years. The scenario analysis reveals an inverse relationship between coefficient of performance (COP) and total energy saved: a larger, more heavily used heat pump lowers the COP (from 3.47 to 2.49 and 2.08) while substantially increasing fossil-fuel displacement (from 59.69 to 119.94 GWh), underlining that absolute primary-energy reduction is the more relevant decarbonisation metric.

Across all three sites two consistent findings emerge. First, the early years of operation are not representative as each system passes through a multi-year transient toward equilibrium, so performance guarantees, recovery efficiencies, and cost estimates must rest on multi-year horizons. Second, the integration of storage into the surface system, like connection topology, component sizing, and control strategy, is as decisive as the storage technology itself. In each case co-simulation made these levers visible and distinguished fundamental limits from integration choices, confirming it as a transferable, practical methodology for assessing high-temperature seasonal storage under realistic operating conditions.

Table of Contents

List of tables

List of figures

List of Abbreviations

Abbreviation	Definition
API	Application Programming Interface
ATES	Aquifer Thermal Energy Storage
BHE	Borehole Heat Exchanger
BTES	Borehole Thermal Energy Storage
CHP	Combined Heat and Power Plant
COP	Coefficient of Performance
DARTS	Delft Advanced Research Terra Simulator
DHN	District Heating Network
Dymola	Dynamic Modelling Laboratory
FDM	Finite Difference Method
FEFLOW	Finite Element subsurface FLOW system
FEM	Finite Element Method
FMI	Functional Mock-up Interface
FMU	Functional Mock-up Unit
HT-ATES	High-Temperature Aquifer Thermal Energy Storage
HT	High Temperature
LCOH	Levelised Cost of Heat
MD	Medium Deep
MTES	Mine Thermal Energy Storage
OWD	Open Warmtenet Delft
RUB	Ruhr University Bochum
TESPy	TESPy (Thermal Engineering Systems in Python)
TUD	Technical University of Delft
UTES	Underground Thermal Energy Storage

1. Introduction

1.1. PUSH-IT project

The Piloting Underground Storage of Heat In geoThermal Reservoirs (PUSH-IT) project is a four-year initiative funded by the European Union's Horizon Europe research and innovation programme, launched in January 2023. The project aims to demonstrate full-scale applications of high-temperature seasonal heat storage (up to 90°C) in geothermal reservoirs across six European sites, covering a range of storage technologies, geological conditions, and societal contexts representative of the broader European energy landscape.

Three core thermal energy storage technologies are developed and tested within the project. Aquifer Thermal Energy Storage (ATES) stores and recovers thermal energy in permeable underground layers containing groundwater. Borehole Thermal Energy Storage (BTES) uses vertically installed tube systems in boreholes to create large underground heat exchangers. Mine Thermal Energy Storage (MTES) utilises water present in abandoned mines as a medium for transporting and storing heat. These technologies are demonstrated at three pilot sites — Delft (Netherlands), Darmstadt (Germany), and Bochum (Germany) — and further developed at three follower sites in Berlin (Germany), Litoměřice (Czech Republic), and United Downs (United Kingdom).

Beyond technology demonstration, PUSH-IT addresses the enabling conditions for widespread deployment: societal engagement, governance frameworks, economic viability, and operational risk reduction. A key strand of this work is the development and application of advanced simulation tools that can assess system performance under realistic operating conditions — of which co-simulation is the central methodology addressed in this deliverable.

1.2. Goals of this report

This report presents the co-simulation work carried out within Task 3.4.2 of Work Package 3 (Enabling Technologies). The primary goal is to document the co-simulation methods developed and applied across the PUSH-IT demonstration sites, present the simulation results for each site, and compile the key lessons learned for future application and optimisation.

Co-simulation, as applied here, refers to the coupled simulation of subsurface thermal storage models and surface-side energy system models, each solved in their respective domain-specific simulators. Each component simulator runs in its native environment and boundary conditions, while exchanging simulation parameters at defined synchronization points at runtime. This approach is necessary to accurately represent the dynamic interactions between the geological storage medium and the district heating infrastructure without sacrificing the numerical fidelity of either domain.

The specific objectives of this report are to:

i) describe the general co-simulation framework and the different technical coupling approaches implemented across the project;

ii) present the site-specific model setups, simulation scenarios, and results for the Darmstadt, Delft, and Bochum demonstration sites; and

iii) distil transferable lessons learned regarding co-simulation methodology, model coupling strategies, and system behaviour that can inform future projects and upscaling efforts.

Following this introduction, Chapter 2 describes the general co-simulation methodology, including the types of underground and surface component models employed, the different technical interfaces used for model coupling, and the time-step synchronization approach. Chapters 3 through 5 then present the co-simulation work for each demonstration site in a consistent structure: simulation goals, scenario definitions, underground and surface model setups, simulation results, discussion, and lessons learned. Chapter 3 covers the Darmstadt BTES site, Chapter 4 the Delft High-Temperature Aquifer Thermal Energy Storage (HT-ATES) site, and Chapter 5 the Bochum MTES site.

2. Co-Simulation methods

2.1. Introduction

Co-simulation is a powerful methodology for the analysis of complex, multi-domain systems in which different physical processes dynamically interact, but are most accurately described by dedicated, domain-specific simulation tools. Forcing all relevant physics into a single monolithic model — typically requires compromises in either physical detail or numerical fidelity. Co-simulation allows each subsystem to be solved by its most appropriate solver, while exchanging boundary conditions at defined synchronization points in time.

Co-simulation has long been established in engineering disciplines such as automotive and aerospace design, where complex multi-physical systems similarly require the concurrent operation of domain-specific solvers. Its adoption in the field of geothermal energy and thermal storage systems is more recent, driven by the increasing complexity of integrated storage and network configurations.

In the context of underground thermal energy storage (UTES) coupled to district heating networks (DHN), the need for co-simulation arises naturally from the fundamentally different character of the processes involved. On the surface side, components like heat pumps, heat exchangers, storage tanks, pumps, and the distribution network operate on timescales of minutes to hours and are governed by thermodynamic and hydraulic equations well-suited to component-based modelling environments. The subsurface, by contrast, involves thermo-hydraulic transport processes in porous or fractured geological media that evolve over days to seasons and require spatially resolved, three-dimensional numerical simulation to be captured with adequate accuracy. As demonstrated by Formhals et al. (2022) [1], accurately resolving the transient load flows of the above-ground installation alongside the detailed heat and mass transport in the geological reservoir is only feasible if both domains retain their native numerical representations, a requirement that co-simulation is specifically designed to fulfil.

Within the PUSH-IT project, co-simulation is a computational framework used for assessing the performance of high-temperature underground seasonal heat storage systems at three demonstration sites (see concept in Figure 1) with different storage technologies: 1) borehole thermal energy storage (BTES) in Darmstadt, 2) aquifer thermal energy storage (ATES) in Delft, and 3) mine thermal energy storage (MTES) in Bochum. Despite the site-specific differences in storage technology and system configuration, the co-simulation approach follows a common logic: a subsurface model captures the geological storage dynamics, while a surface-side model represents the energy system and network, and the two are coupled through a defined interface that synchronizes boundary conditions at each time step.

The following sections describe the model types used for the underground and surface domains, the different technical approaches implemented for inter-model communication, and the time-step synchronization strategy applied across all sites.

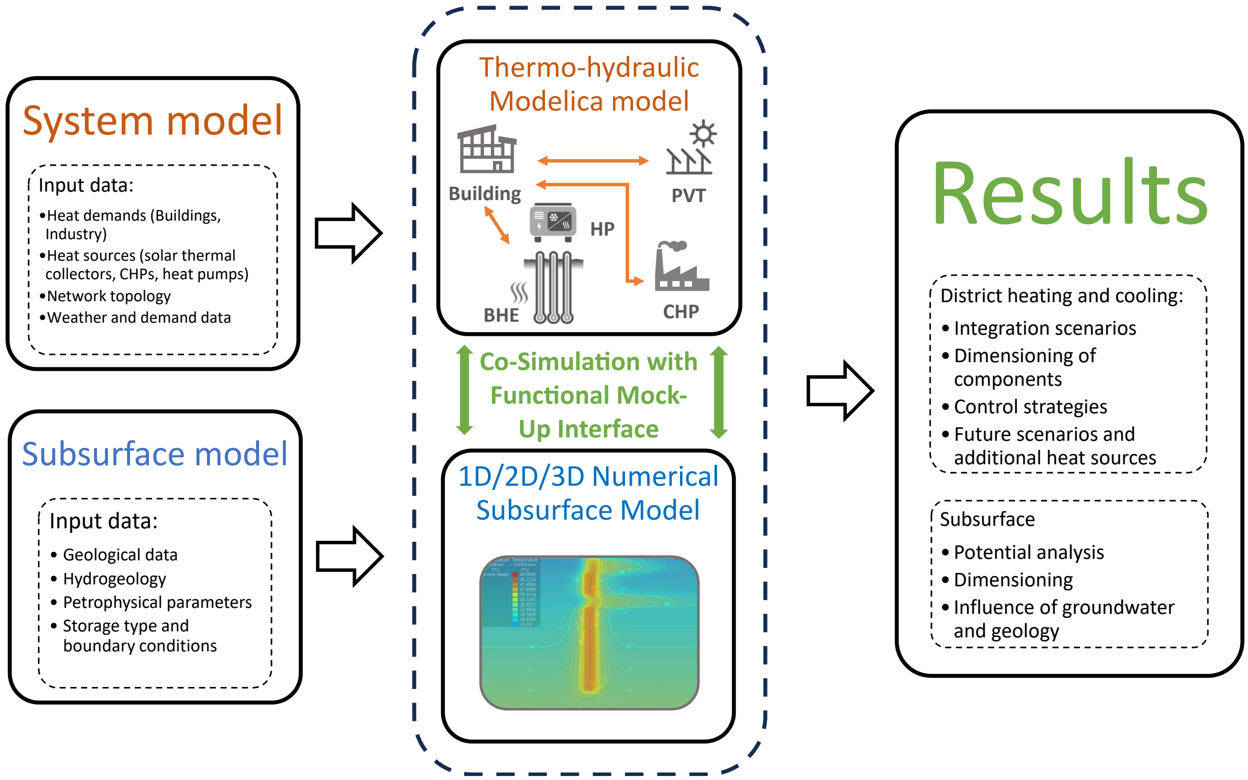

Figure 1: Co-simulation scheme for coupling district heating network models and 3D FEM models with system-specific inputs and results

2.2. Underground thermal energy storage models

2.2.1. General modelling approaches for underground thermal energy storage

Simulating the subsurface dynamics of underground thermal energy storage systems requires the numerical representation of coupled flow and heat transport processes in geological media. The governing physics are well established: fluid flow in porous or fractured media is described by Darcy's law, which relates the fluid flux to the hydraulic gradient through the permeability of the medium. Heat transport in the subsurface is governed by the coupled advection-conduction equation, accounting for heat carried by the moving fluid as well as conductive heat transfer through both the solid matrix and the pore fluid. In systems with significant temperature gradients or high injection temperatures, buoyancy-driven flow due to thermally induced density differences may also play an important role and must be captured by the model.

The governing equations for groundwater flow and heat transport are solved numerically using a range of approaches. Finite element methods (FEM) and finite difference methods (FDM) are the most widely used, offering flexible spatial discretisation and the ability to discretise complex geometries and heterogeneous subsurface conditions. For BTES systems, where heat transfer occurs primarily through conduction between the borehole heat exchanger and the surrounding rock, dedicated analytical and semi-analytical approaches – such as the infinite line source model or its extensions – have historically been used for long-term performance assessment. However, when the thermal plume interacts with groundwater flow, when the borehole field geometry is complex, or when dynamic coupling to a surface energy system is required, fully numerical three-dimensional models are necessary.

For ATES systems, the three-dimensional spatial distribution of the thermal plume in the aquifer and its sensitivity to groundwater flow, thermal stratification, and buoyancy effects make full numerical simulation the standard approach. For MTES, the typical modelling approach combines a three-dimensional representation of the surrounding rock mass with discrete lower-order elements – commonly one-dimensional pipe or channel elements, or two-dimensional planar elements – representing the mine shafts and galleries explicitly within the 3D domain. This hybrid strategy acknowledges that the void spaces of the mine have fundamentally different hydraulic and thermal characteristics from the porous rock matrix and are better described by dedicated flow and heat transfer formulations. However, applying even this approach requires a sufficiently detailed knowledge of the mine geometry, the hydraulic connectivity between workings, and the thermal properties of the surrounding rock.

2.2.2. Site specific UTES simulators

For the Darmstadt BTES site, the subsurface is modelled using FEFLOW (Finite Element subsurface FLOW system) [2], a commercial finite-element software for the simulation of flow and heat transport in porous and fractured media. The FEFLOW model resolves the three-dimensional thermo-hydraulic behaviour of the borehole field and the surrounding crystalline rock mass in full spatial detail, capturing the evolution of the subsurface temperature field over seasonal cycles. This level of resolution is justified by the relatively well-characterised geology of the site and the need to accurately represent heat conduction and storage dynamics in the deep borehole field.

For the Delft ATES site, the subsurface is represented by DARTS (Delft Advanced Research Terra Simulator) [3], a high-performance reservoir simulation framework developed at TU Delft. DARTS provides a fully three-dimensional representation of the aquifer, capturing the coupled thermal and hydraulic processes governing heat injection, storage, and recovery in the target formation. The Delft co-simulation is described in detail in Chapter 4.

For the Bochum mine water site, the situation is fundamentally different. Unlike aquifer or borehole systems, abandoned mine workings present a highly complex, partially unknown geometry with limited available characterisation data. At the time of this work no validated three-dimensional numerical model of the mine thermal system exists, nor would the current state of site knowledge justify the construction of one. Building a spatially resolved FEM model on the basis of uncertain geometry and poorly constrained thermal and hydraulic parameters would introduce a false sense of precision without a corresponding gain in predictive reliability. The underground component for Bochum is therefore represented by a low-order, physics-based model implemented in Python, capturing the essential thermal storage and heat transfer behaviour of the mine water system through a set of governing energy balance equations. This approach is both commensurate with the available site knowledge and well-suited to the exploratory character of the Bochum co-simulation, which aims to assess system behaviour and sensitivity rather than produce site-specific predictions.

2.3. Energy system models

The surface-side energy system encompasses all components that generate, distribute, store, and consume thermal energy above ground — including heat sources, heat pumps, buffer storage tanks, circulation pumps, control systems, and the district heating network itself. Simulating this side of the coupled system requires tools capable of resolving transient thermodynamic and hydraulic behaviour across a network of interconnected components, driven by time-varying heat sources, demands, and control signals.

Energy system modelling in this context is typically approached through equation-based or flow-network modelling frameworks. In component-based environments, each component is described by a set of differential and algebraic equations governing mass and energy balances, and the full system is assembled by connecting components through shared variables — typically mass flow rate, supply and return temperatures, and pressure. This approach handles the bidirectional propagation of information through the network and allows complex control strategies to be implemented directly within the model. Flow-network approaches, by contrast, decompose the system into nodes and edges and solve mass and energy balances iteratively, offering computational efficiency for large networks at the cost of some flexibility in component representation.

In the PUSH-IT project, two complementary modelling environments are used for the energy system side of the co-simulation, reflecting the different site configurations and modelling objectives.

1. Modelica [4] is an equation-based, object-oriented modelling language well-established for the simulation of complex multi-domain physical systems. Models are constructed by connecting component models from standardised libraries, with the system equations assembled and solved simultaneously by a Modelica-compliant simulation environment. For the PUSH-IT co-simulation work, two open-source Modelica libraries form the foundation of the energy system models. The Modelica Buildings Library [5] provides a broad collection of validated component models for building energy systems, including heat pumps, heat exchangers, fluid circuits, and controllers. DisHeatLib [6] extends this with components specifically developed for district heating applications, including district heating network elements, substation models, and thermal storage components. Together, these libraries enable the construction of detailed, physically consistent models of the full energy system — from the thermal storage interface to the district heating distribution network and end consumers — for the Darmstadt BTES and Bochum MTES sites.
2. TESPy (Thermal Engineering Systems in Python) [7] is an open-source Python-based framework for the steady-state and transient simulation of thermal engineering systems using a flow-network approach. Components such as heat exchangers, turbines, pumps, and piping are connected through a network topology, and the system of energy and mass balance equations is solved iteratively. TESPy is used for the surface-side energy system model at the Delft ATES site, where it is coupled to the DARTS subsurface simulator.

2.4. Inter-model coupling approaches

2.4.1. Python Interfaces

Several professional and open-source subsurface simulation environments expose a Python Application Programming Interface (API) that allows external scripts to interact directly with the simulator at runtime, reading state variables, setting boundary conditions, triggering time step advances, and retrieving results without the need for file-based data exchange or intermediate coupling middleware. This makes Python scripting a particularly flexible and transparent coupling mechanism, as the full coupling logic, control strategy, and data exchange can be implemented in a single Python orchestration script that drives both simulators in a coordinated manner.

In the PUSH-IT project, Python APIs are used as the primary coupling mechanism at two sites. FEFLOW, the finite-element subsurface simulator used for the Darmstadt BTES site, exposes its functionality through the Interface Manager Python API, which allows external Python scripts to control the simulation, access nodal temperatures and fluxes, and modify boundary conditions at each coupling time step. At the Delft ATES site, OpenDARTS provides a native Python interface through which the reservoir simulation is embedded directly within the Python co-simulation environment.

A particularly direct case of Python-based coupling arises at the Bochum MTES site, where the underground thermal storage model itself is implemented as a set of physics-based equations in Python. Here, no inter-process communication is required between separate simulator instances since the subsurface model and the orchestration logic coexist within the same Python environment, and data exchange is handled through direct function calls. This approach offers maximum transparency and computational efficiency, at the cost of being limited to low-order model representations.

2.4.2. Functional Mock-up Interface

The Functional Mock-up Interface (FMI) [8] is an open standard for the exchange and co-simulation of dynamic models across different simulation tools. A model exported according to the FMI standard is packaged as a Functional Mock-up Unit (FMU) – a self-contained binary that encapsulates the model equations, state variables, and a standardised interface through which an external master algorithm can initialise the model, set inputs, advance the simulation by one time step, and retrieve outputs. FMI has become widely adopted in industrial and research simulation workflows, particularly for model exchange between equation-based environments and other simulation platforms.

In the PUSH-IT project, the Modelica energy system models for the Darmstadt and Bochum sites are exported as FMUs and integrated into the Python-based co-simulation orchestration layer. This allows the Modelica surface model to be advanced step-by-step in synchrony with the subsurface model, with boundary conditions — such as inlet temperatures and mass flow rates at the storage interface — exchanged at each coupling time step. The FMI-based approach thus bridges the Modelica modelling environment and the Python coupling infrastructure in a standardised and tool-independent manner.

3. Darmstadt site

3.1. Goals of Co-Simulation

The co-simulation approach for the Darmstadt demonstration site serves a highly specific, diagnostic purpose. The demonstration site features three 750 meter Medium-Deep Borehole Heat Exchangers connected to the Mechanical Engineering faculty sub-grid of the TU Darmstadt district heating network (Figure 2). While the injection of heat (charging) into the borehole thermal energy storage (BTES) has been successfully demonstrated in practice, multiple challenges have prevented the successful extraction of this heat (discharging). These challenges are partly related to the connection point, the seasonal warm weather during the discharge operation as well as the energy consumption, which has been reduced as a result of energy-saving and renovation measures, so that the performance metrics at the transfer point differed significantly between the planning phase and the operation phase.

Therefore, the primary goal of the co-simulation, which couples a FEFLOW subsurface model with a Modelica-based surface energy system model, is to dynamically replicate this bottleneck and identify what is technically and operationally required to achieve successful discharging.

While the surface energy system model is a behavioural representation rather than an exact, component-for-component digital twin of the real-life infrastructure, it accurately captures the fundamental thermo-hydraulic constraints of the system. By isolating variables such as mass flow rates, heat exchanger effectiveness, and specifically the temperature lifts required by the heat pumps, the simulation demonstrates the thermodynamic boundaries of the current setup. The goal is to show why the current configuration misses to fully discharge the storage and providing, what architectural or control-logic modifications are necessary to make the system operate as a functional seasonal thermal energy storage.

3.2. Simulation scenarios

To systematically diagnose the discharge issue and evaluate potential solutions, the simulation investigates the thermo-hydraulic behaviour of the BTES when integrated directly into the Mechanical Engineering sub-grid of the TU Darmstadt district heating network. The investigation focuses on the hydraulic connection points and is divided into two primary scenarios:

- Base Scenario (Current Case): This scenario directly replicates the existing physical infrastructure. In this configuration, the BTES is connected directly to the sub-grid with the intention of discharging stored heat by pre-heating the return flow immediately after an individual building's substation. After passing the BTES heat exchanger, this locally heated fluid merges into the central return line heading back to the Combined Heat and Power (CHP) plant. This scenario is used to diagnose the specific local thermodynamic constraints, such as temperature levels and mass flow rates at this specific building node, which are currently preventing effective heat extraction.
- Optimized Scenario (Ideal Case): This scenario alters the hydraulic topology of the surface-side infrastructure to test a more favourable integration strategy. While the BTES remains directly connected to the sub grid, the connection point is relocated from the individual building to the main central return pipe, positioned downstream of all buildings within the Mechanical Engineering sub grid. By shifting the integration point, this scenario evaluates whether the aggregated return flow provides the necessary temperature differentials and mass flow stability to successfully discharge the stored heat and return it to the CHP plant.

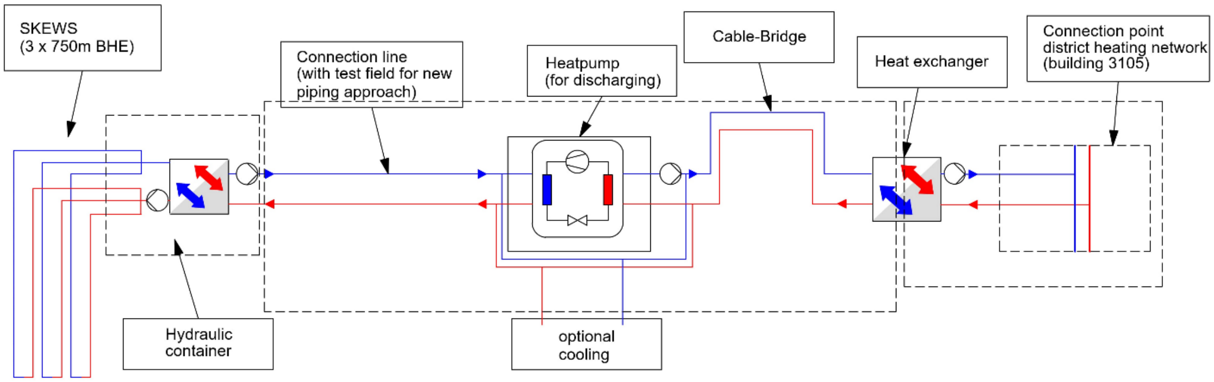

Figure 2: Hydraulic connection scheme of the MD-BTES at the sub grid of the mechanical engineering buildings

3.3. Underground model setup

The subsurface domain for the Darmstadt site is represented using a fully coupled, three-dimensional thermo-hydraulic numerical model built in FEFLOW 10.0 (Figure 3). The primary objective of this model is to accurately capture the spatial distribution of temperatures and the conductive heat transfer between the three 750 m Medium-Deep Borehole Heat Exchangers (MD-BHE) and the surrounding crystalline rock mass.

3.3.1. Meshing and Geometry

A defining characteristic of the Darmstadt installation is the specific trajectory of the boreholes. Rather than being perfectly vertical, the three MD-BHEs deviate from their surface origin. To accurately represent these measured, deviated bore paths within the numerical domain, an unstructured mesh was generated using a combination of the external tool MeshIt [9] and the native meshing features of FEFLOW 10.0.

To ensure numerical stability and to correctly resolve the steep thermal gradients near the heat exchangers, the spatial discretization was highly refined around the boreholes. The distance between the BHE nodes was constrained to 1 m along the borehole axis. In the horizontal plane, six auxiliary help nodes were placed around each BHE at a radial distance of 0.74 m, following established specific distance factor methodologies. The resulting system of equations was solved using the PETSc Krylov Subspace Method (KSP) solver.

3.3.2. Geological Model and Parameters

The local geology was simplified into a three-layer model representing the dominant rock units (Table 1) encountered during drilling: Basalt, Lichtwiese Granite, and Darmstadt Granodiorite. While the model assumes fully saturated groundwater conditions, groundwater flow (advection) was explicitly disabled. This decision was made to isolate the effects of conductive heat transfer and borehole path deviation without the complicating influence of regional groundwater movement.

The thermal and hydraulic properties assigned to these units were derived from a combination of cutting analysis, outcrop studies, and regional databases. The baseline temperature field was initialized based on temperature logging from the site, which indicated a local geothermal gradient of 23 K km^{-1}. Prior to the transient co-simulation, a steady-state run was performed using Dirichlet boundary conditions for hydraulic head and temperature to establish the initial subsurface conditions.

Table 1: Assigned geological properties in the FEFLOW model

Rock Unit	**Depth [m]**	**Thermal Conductivity [W m^{-1} K^{-1}]**	**Volumetric Heat Capacity [MJ m^{-3} K^{-1}]**	**Porosity [-]**	**Hydraulic conductivity [m s^{-1}]**
Basalt	0 – 160	1.9	1.95	0.07	1.15e-04
G1 Granite	160 – 430	2.6	2.19	0.026	6.50e-06
Granodiorite	430 – 1000	3.3	2.22	0.005	5.00e-08

3.3.3. BHE Configuration

The three boreholes are configured as coaxial central inlet (CXC) heat exchangers. Due to input limitations within the FEFLOW environment, the complex composite geometry of the real-world pipes was simplified. The model applies an effective thermal conductivity of 0.4 W m^{-1} K^{-1} to represent the inner composite pipe (Polypropylene Random Copolymer, and steel). The outer annulus is filled with a highly conductive geothermal grout assigned a thermal conductivity of 3.0 W m^{-1} K^{-1} along the entire length of the borehole, excluding the low-conductivity upper section (0 – 150 m) since FEFLOW allows only for one grout section. The heat transfer between the circulating fluid and the rock mass is calculated using the quasi-stationary Eskilson and Claesson analytical method.

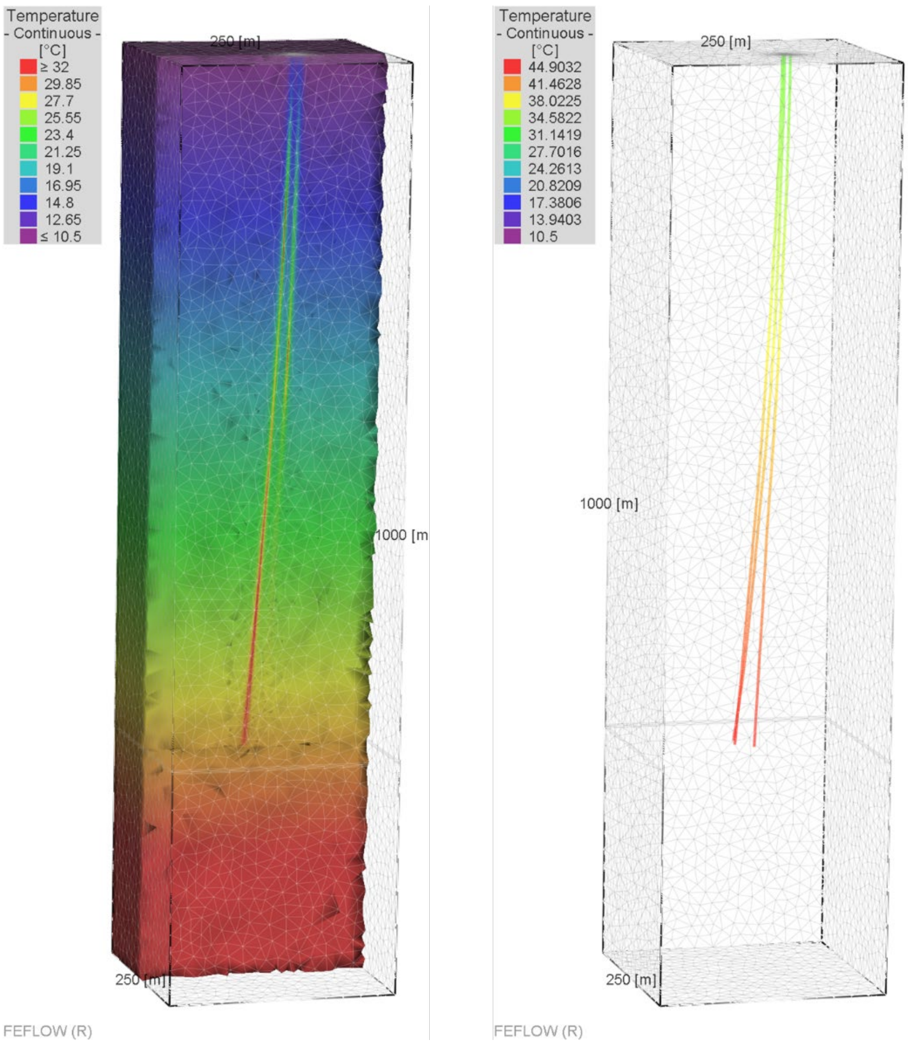

Figure 3: 3D-FEM model of the 3 deviated borehole heat exchangers at the Darmstadt demo site

3.4. Surface components model setup

The surface-side energy system for the Darmstadt site is modelled in Modelica using the Buildings library, implemented in the Dynamic Modelling Laboratory (Dymola) simulation environment (Figure 4). The model captures the transient thermodynamic and hydraulic behaviour of the full above-ground system over a multi-year simulation horizon, including fluid circuits, heat exchangers, heat pump, control logic, and the connection to the district heating network.

The model distinguishes two hydraulically separated fluid circuits. The BTES loop circulates the heat transfer fluid through the borehole field and connects to the surface plant via a heat exchanger, while the district heating loop carries network water between the surface plant and the campus grid. To represent the thermal inertia and heat losses of the physical installation, the approximately 130-metre transport distance between the borehole field and the mechanical plant room is modelled using buried plug-flow pipe components with ground coupling, ensuring that the temperatures arriving at the heat exchangers reflect realistic environmental conditions rather than idealised boundary assumptions.

Heat transfer between the two fluid circuits is handled by a heat exchanger which physically and hydraulically decouples the BTES loop from the district heating side. A Carnot-based heat pump model with a nominal heating capacity of 293 kW and a Carnot efficiency factor of 0.4 is integrated on the district heating side to bridge the temperature gap between the heat recovered from the borehole field and the 75 °C supply temperature required by the campus grid. During discharge operation, the heat pump draws from the BTES heat exchanger output at its evaporator and upgrades it to meet this supply temperature requirement.

The boundary conditions of the model are derived from measured time-series data from the TU Darmstadt campus, including historical heat demand profiles and the dynamic supply and return temperatures of the connected campus sub grid. This ensures that the surface model responds to realistic operational conditions rather than synthetic load assumptions.

The operational control is implemented as a rule-based state machine with three modes: charge, discharge, and storage. Charging is restricted to a defined summer window, from approximately the beginning of May to the end of September, during which surplus heat from the campus is injected into the borehole field. Discharge is only permitted if a preceding charging phase has been completed and is subject to a temperature-based safety lockout: if the fluid temperature at the BTES outlet falls below 13 °C, discharge is suspended and the system returns to storage mode to protect the heat pump evaporator and prevent excessive thermal depletion of the subsurface. Hydraulic switching between operational modes is managed by a set of two-way control valves and flow-controlled circulation pumps, which redirect mass flows according to the active system state.

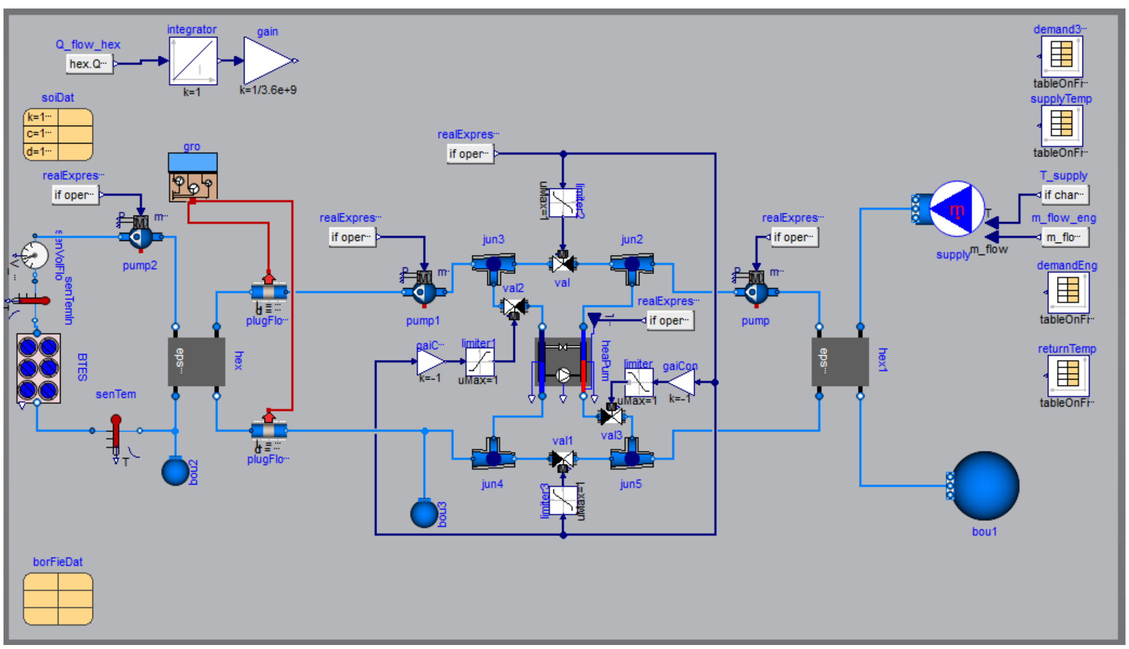

Figure 4: Modelica model of the Darmstadt surface-side energy system implemented in Dymola. The model comprises the BTES loop (left) with borehole field, circulation pump, temperature sensors, and plate heat exchanger, the central heat pump unit, and the district heating connection (right) with plug-flow transport pipes, control valves, and flow-controlled pumps

3.5. Simulation results

The co-simulation was run over six consecutive operating years for both the current and ideal scenarios, allowing the seasonal charge-discharge behaviour of the BTES to develop from cold initial conditions toward a thermally quasi-steady state. Results are presented in terms of the borehole field inlet and outlet temperatures, the annual heat budget, and the recovery efficiency. Additionally, the co-simulation results are compared against a standalone Modelica simulation using the built-in Buildings Library bore field model to assess the validity of using a simplified subsurface representation.

3.5.1. Thermal behaviour of the BTES

Figure 5 shows the BTES inlet and outlet temperatures over the full simulation period for both the current and ideal coupling configurations. In both cases, the seasonal charge-discharge pattern is clearly visible: inlet temperatures rise to approximately 80 °C during the summer charging period and drop sharply at the onset of the winter discharge phase. The outlet temperature response, however, differs considerably between the two scenarios, where there is virtually no heat extraction in the current implementation and only marginal extraction in the optimised scenario. In both scenarios the storage is charged at high temperature but discharged at a low temperature and a small temperature difference, so only a small fraction of the stored heat is recovered.

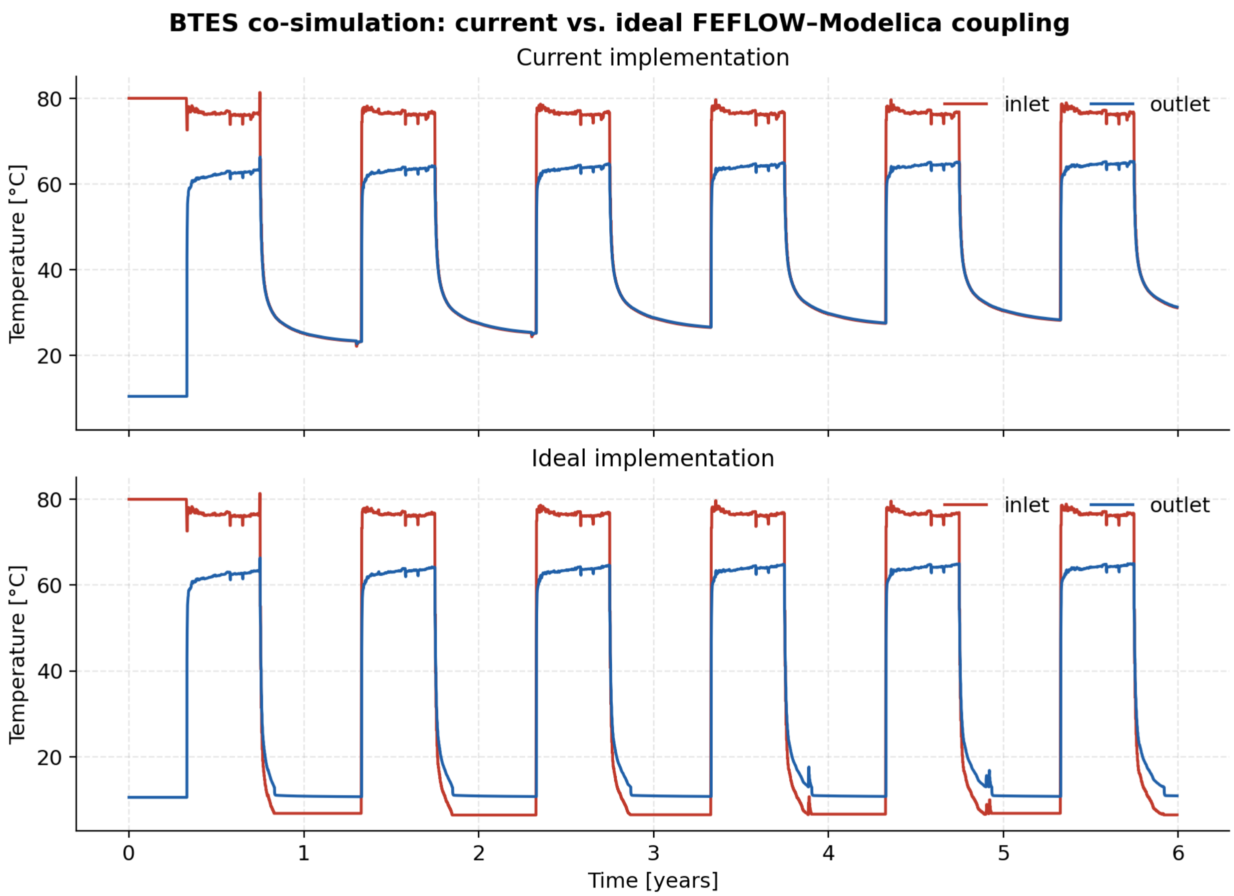

Figure 5: BTES inlet and outlet fluid temperatures over six operating years for the current (upper panel) and ideal (lower panel) FEFLOW–Modelica co-simulation scenarios

In the current scenario (upper panel), the outlet temperature during discharge remains consistently elevated, staying above approximately 23 °C throughout the discharge period and never reaching the low values that would indicate effective heat extraction from the subsurface. This behaviour is a direct consequence of the hydraulic boundary conditions at the individual building connection point: the local return flow temperature and mass flow rate are insufficient to create the driving temperature differential needed for effective discharge through the heat exchanger. As a result, the BTES continues to accumulate heat cycle after cycle without recovering a meaningful fraction of the stored energy and heat is only transferred through circulation losses in the connection line.

In the ideal scenario (lower panel), the discharge behaviour is different. The outlet temperature drops sharply at the start of each discharge phase, reaching values near 10 °C in later operating years, and the inlet temperature similarly falls to low values during discharge, reflecting full utilisation of the available temperature differential at the central return pipe connection point. The progressive stretching of the discharge period across successive years reflects the thermal evolution of the BTES as it gets more efficient over the simulation time.

3.5.2. Heat budget and recovery efficiency

The annual heat budget for both scenarios, presented in Figure 6 and Figure 7, quantifies the contrast in system performance between the two hydraulic configurations.

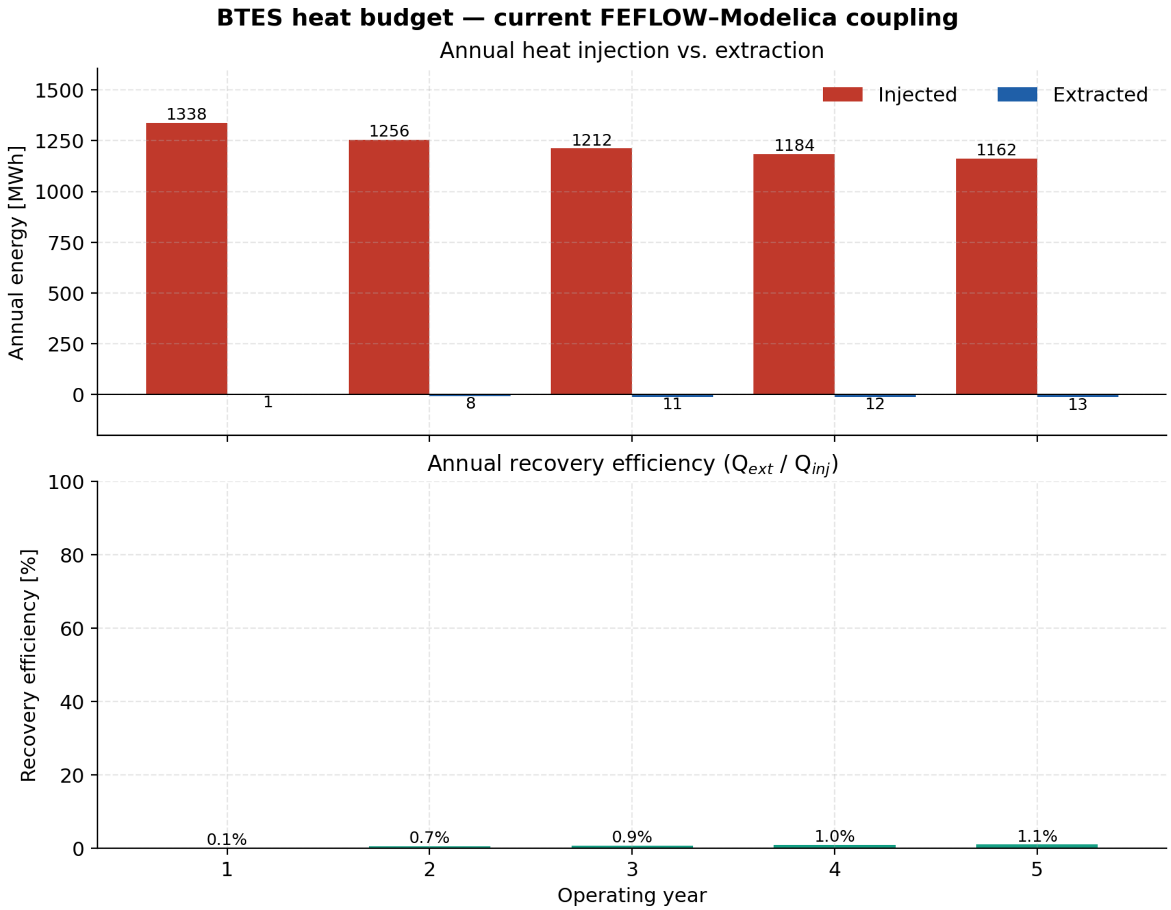

Figure 6: Annual heat budget for the current FEFLOW–Modelica co-simulation scenario, showing heat injected into and extracted from the BTES field per operating year (upper panel) and the corresponding annual recovery efficiency (lower panel)

In the current scenario, heat injection into the BTES field declines gradually from 1338 MWh in year one to 1162 MWh in year five, consistent with progressive thermal saturation of the subsurface. Heat extraction, however, remains negligible throughout the simulation period, rising only from 1 MWh to 13 MWh over five years, corresponding to recovery efficiencies between 0.1% and 1.1%. These values confirm that the current hydraulic integration effectively renders the BTES non-functional as a seasonal discharge system under the simulated conditions.

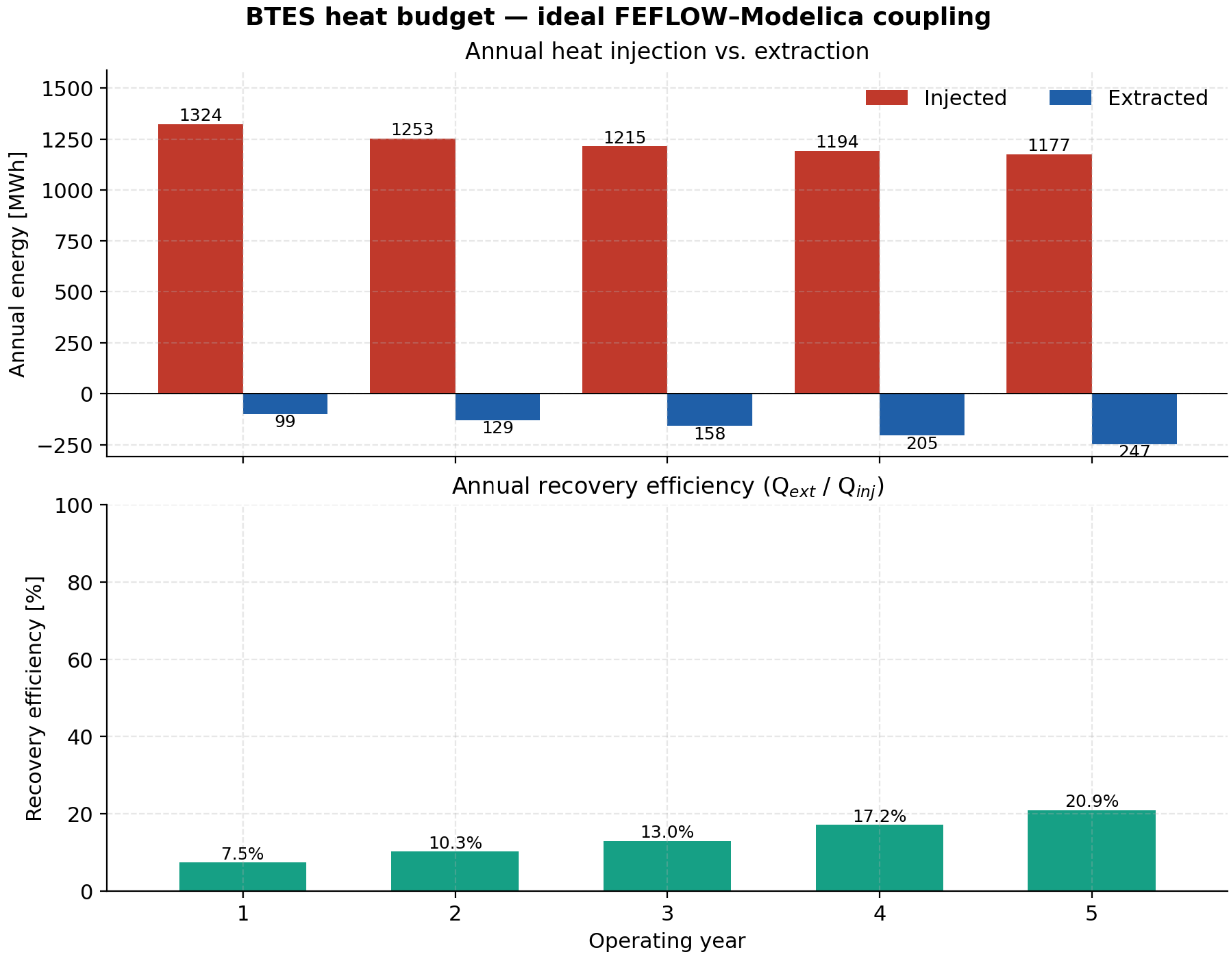

Figure 7: Annual heat budget for the ideal FEFLOW–Modelica co-simulation scenario, showing heat injected and extracted per operating year (upper panel) and the annual recovery efficiency (lower panel)

In the ideal scenario, the same declining injection trend is observed – from 1324 MWh in year one to 1177 MWh in year five – while heat extraction increases substantially with each operating year, growing from 99 MWh to 247 MWh. The corresponding recovery efficiency rises from 7.5% in the first year to 20.9% by year five, reflecting both the improving thermal state of the field and the growing effectiveness of discharge as the subsurface temperature builds up over successive charging seasons. The upward trend in recovery efficiency has not yet plateaued by the end of the simulation, suggesting that further improvement is expected as the system approaches a fully periodic steady state.

It should be noted that the absolute recovery efficiencies remain relatively modest even in the ideal scenario. This is partly a consequence of the early stage of system operation – the borehole field requires multiple charge-discharge cycles to reach thermal equilibrium – and partly attributable to the currently small number of installed BHE compared to their depth.

3.5.3. Subsurface temperature distribution

The spatial temperature distribution at 750 m depth within the BTES field, as simulated by the FEFLOW model of the ideal scenario, is shown in Figure 8 for the end of the charging and discharging phases in operating year five. At the end of the charging phase, the thermal influence is concentrated in tight, high-temperature zones immediately surrounding the individual borehole locations, with peak temperatures exceeding 50 °C at the borehole walls and a relatively limited lateral extent of the elevated temperature region into the surrounding crystalline rock mass. This pattern reflects the predominantly conductive heat transport regime in the low-permeability granodioritic reservoir, where heat spreads slowly outward from the boreholes without advective transport.

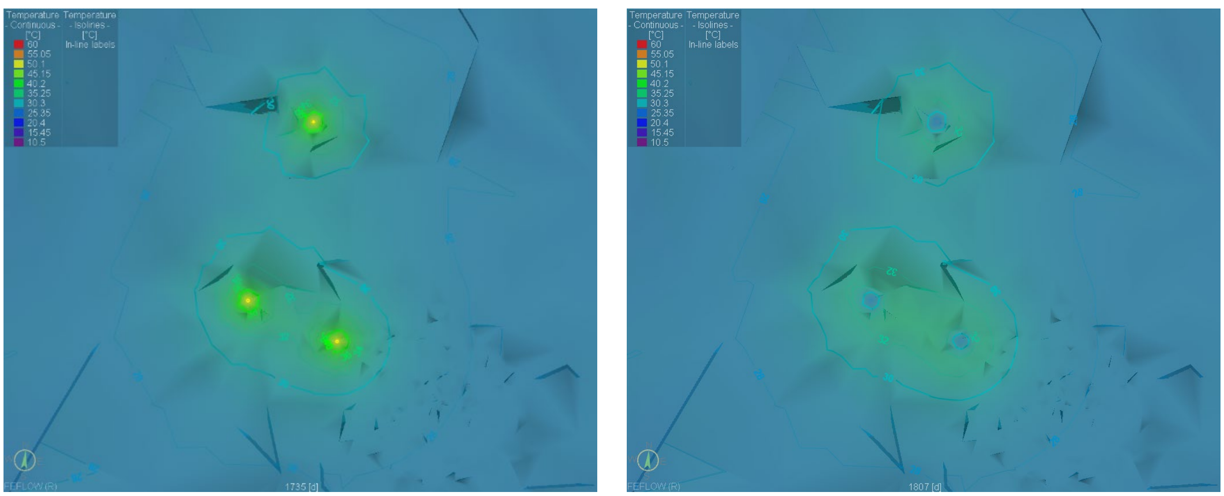

Figure 8: Simulated subsurface temperature distribution in the BTES field (depth of 750 m) at the end of the charging phase (left) and end of the discharging phase (right) in operating year five, as computed by the FEFLOW finite-element model

3.5.4. Comparison with the standalone Modelica bore field model

Figure 9 shows a comparison of the BTES inlet and outlet temperatures between the ideal FEFLOW co-simulation and a standalone Dymola simulation using the built-in Buildings Library two-U-tube bore field model calibrated to the measured borehole resistance values of the demonstrator implementation.

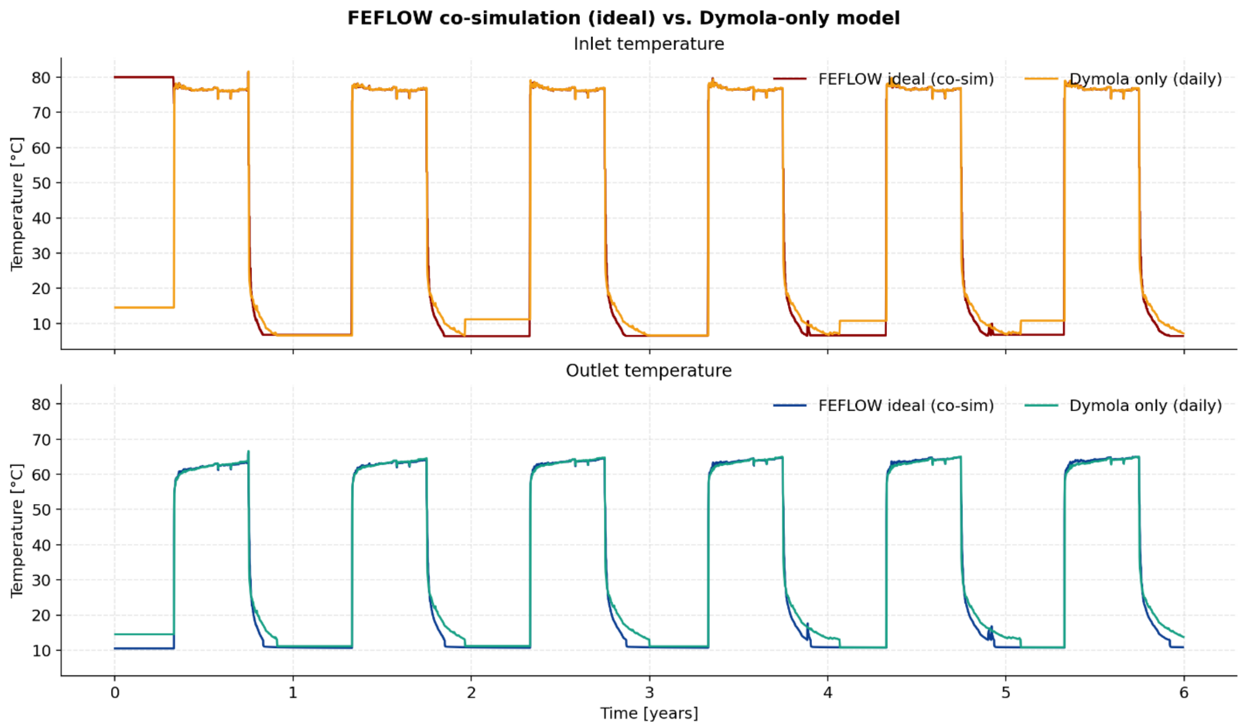

Figure 9: Comparison of BTES inlet (upper panel) and outlet (lower panel) temperatures between the ideal FEFLOW co-simulation and a standalone Dymola simulation using the Buildings Library bore field model over six operating years

The inlet temperatures produced by both approaches are in close agreement throughout the simulation period, confirming that the surface-side control logic and heat source behaviour are consistent between the two model configurations. The outlet temperatures show a generally good correspondence, with the Dymola-only model reproducing the seasonal charge-discharge pattern and the progressive temperature evolution of the field. Some divergence is visible particularly during the discharge phase in later years, where the Dymola bore field model produces slightly higher outlet temperatures than the FEFLOW co-simulation. This discrepancy likely reflects the simplified representation of the subsurface in the bore field model, which does not capture the full three-dimensional thermal field and may underestimate heat losses to the surrounding rock. Nevertheless, the overall agreement supports the use of the simplified Modelica bore field representation for rapid scenario screening, while the FEFLOW co-simulation remains necessary for spatially resolved analysis and accurate long-term performance assessment.

3.5.5. Upscaled implementation

An upscaling of the Darmstadt field has been foreseen as a possible future development stage, increasing the number of borehole heat exchangers from three to either 19 or 37. The 37-BHE configuration was implemented and simulated here, retaining the three existing deviated boreholes and adding 34 further BHE drilled directionally to planned, regular trajectories rather than inheriting the deviation of the original boreholes. On the surface side, the larger field requires a heat pump in the MW range; a 4 MW unit was used, drawing from the BTES until the borehole outlet temperature falls to a 20 °C cut-off. The associated discharge flow rates of approximately 74 L s^{-1} would in practice require a dedicated connection to the main ring of the district heating network rather than the sub grid integration used at the current scale.

The annual heat budget and recovery efficiency for the upscaled field are shown in Figure 10. After the first-year transient, heat injection stabilises at approximately 11,400 MWh, while heat extraction increases steadily from 5,329 MWh to 8,557 MWh over five operating years. The recovery efficiency rises from 36.5 % in the first year to 74.8 % by year five, with the year-on-year increments diminishing toward the end of the period, indicating that the field is approaching a periodic steady state. This is a fundamentally different performance regime from the three-BHE ideal case, where recovery efficiency reached only 20.9 % after five years and had not begun to plateau. The improvement follows directly from the scaling of the field. The larger borehole array reduces the surface-area-to-volume ratio of the heated rock mass and increases the thermal interaction between boreholes, so that a greater fraction of the injected heat is retained within the storage volume and recovered during discharge rather than lost conductively to the surrounding rock. At this scale the field operates as a functional seasonal storage, with extracted energy becoming comparable in magnitude to injected energy.

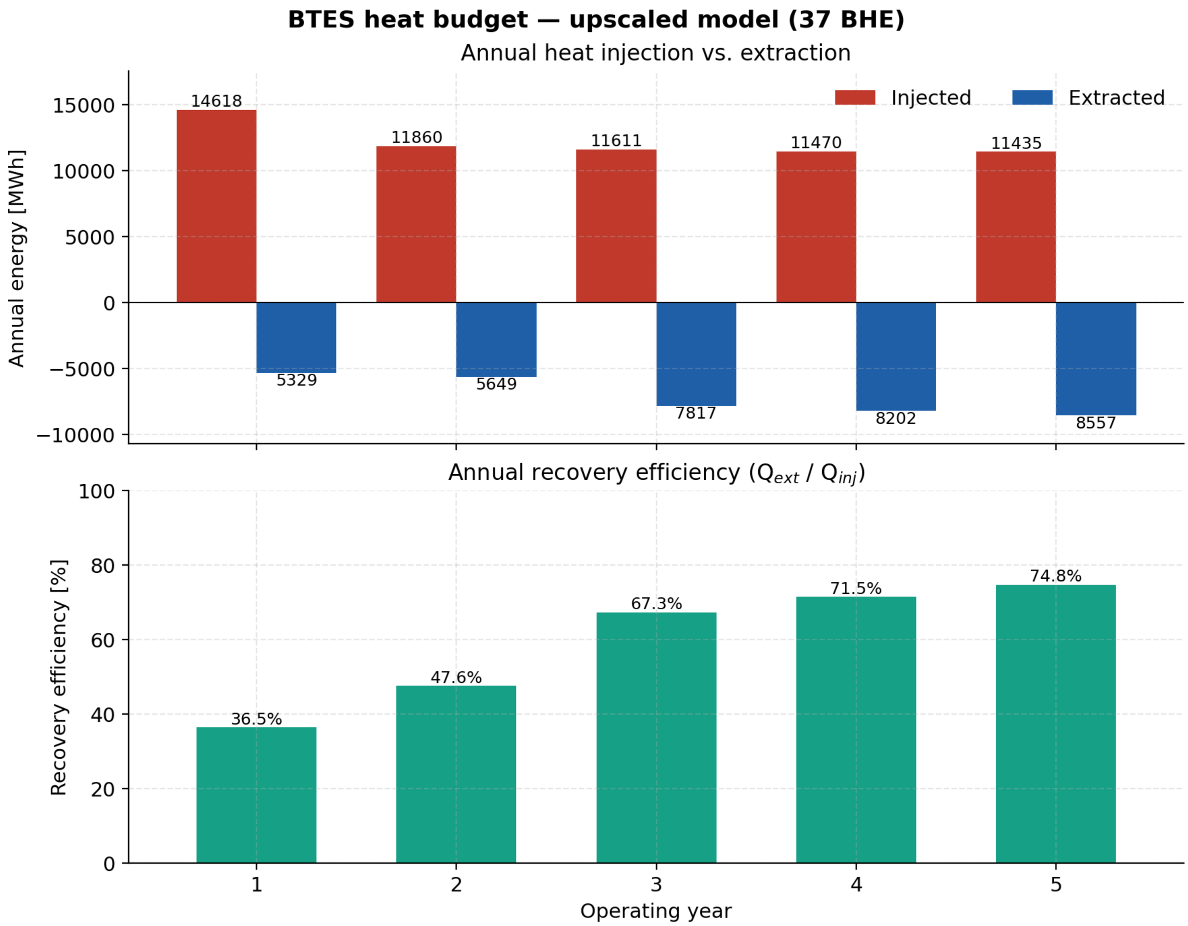

Figure 10: Annual heat budget for the upscaled (37-BHE) FEFLOW–Modelica co-simulation scenario, showing heat injected and extracted per operating year (upper panel) and the annual recovery efficiency (lower panel)

3.6. Discussion

The simulation results reveal that the hydraulic integration point is a key decisive factor governing the BTES discharge performance under the current system configuration. In the current scenario, the connection of the BTES heat exchanger downstream of an individual building substation results in local return flow temperatures and mass flow rates that are insufficient to establish the temperature differential required for effective heat extraction. The BTES consequently operates almost exclusively in charging mode, accumulating heat season after season with negligible recovery, despite the subsurface temperature field clearly demonstrating that substantial thermal energy is stored in the borehole field. This is not a fundamental limitation of the BTES technology itself, but a consequence of the hydraulic boundary conditions imposed by the current connection topology. The ideal scenario confirms this interpretation: relocating the connection point to the central return pipe, where aggregated mass flow rates are higher and return temperatures are more stable, is sufficient to enable meaningful discharge. This finding has direct practical relevance for the planned future development of the Darmstadt site, where the BTES will be reconnected to supply a building directly rather than pre-heating a return line, a configuration that is expected to resolve the discharge limitation identified here.

The recovery efficiencies achieved in the ideal scenario – rising from 7.5% in the first operating year to 20.9% by year five – are consistent with expectations for a system of this configuration at this stage of operation. The Darmstadt BTES comprises only three borehole heat exchangers, which limits the thermal interaction volume and reduces the system's ability to recover heat rapidly during the discharge season. Furthermore, the three boreholes exhibit a borehole path deviation reflecting differences in local geological conditions or borehole completion that additionally limits the thermal interaction between them. Under these conditions, recovery efficiency is expected to improve progressively over multiple operating years as the thermal state of the field builds up toward a quasi-periodic equilibrium, and the upward trend in recovery efficiency observed across the five simulated years is consistent with this behaviour. The upscaled implementation (Section 3.5.5) confirms that the field size is the dominant constraint: increasing the number of borehole heat exchangers to 37 raises the fifth-year recovery efficiency from 20.9 % to 74.8 % under otherwise identical subsurface and hydraulic conditions, and the field approaches a periodic steady state within the simulated period rather than continuing to climb. This demonstrates that the modest efficiencies of the three-BHE configuration are a consequence of limited field size and thermal interaction volume, not a limitation of the storage concept or the chosen integration topology.

The comparison between the FEFLOW co-simulation and the standalone Modelica bore field model demonstrates that the simplified analytical representation captures the principal seasonal dynamics of the system with reasonable fidelity, particularly with respect to charging behaviour and peak outlet temperatures. The divergence observed during the discharge phase in later operating years, where the Dymola bore field model tends to overestimate outlet temperatures relative to the FEFLOW co-simulation, is consistent with the known limitations of analytical bore field models in representing the full three-dimensional thermal field under asymmetric or partially discharged conditions. Nevertheless, the overall agreement is sufficient to support the use of the simplified model for rapid scenario screening and parametric studies, where computational efficiency is prioritized over spatial resolution.

3.7. Lessons learnt

The co-simulation study of the Darmstadt BTES site yields several transferable lessons for the design and operation of BTES systems integrated into district heating networks.

The hydraulic connection point is critical for discharge performance. Pre-heating the return flow of an individual building substation imposes unfavourable boundary conditions, insufficient mass flow and inadequate temperature differential, that effectively prevent heat extraction even when substantial energy is stored in the subsurface. Connecting the BTES at a point with higher aggregated return flow rates and lower, more stable return temperatures is a prerequisite for effective seasonal discharge. System designers should evaluate the hydraulic integration topology as a primary design parameter rather than a secondary installation detail.

Higher flow rates and lower return temperatures on the network side are necessary conditions for effective BTES discharge, if the BTES lifts the return flow temperature. This has implications not only for connection point selection but also for the control strategy of the broader district heating network, where measures that reduce return temperatures directly enhance the potential for BTES heat recovery.

The standalone Modelica bore field model is a useful tool for rapid prototyping and scenario screening but tends to overestimate discharge performance relative to the full three-dimensional FEFLOW co-simulation. This overestimation is most pronounced in later operating years and during the discharge phase, where the simplified subsurface representation cannot capture the spatial heterogeneity of the thermal field. Co-simulation with a spatially resolved subsurface model is therefore recommended where accurate long-term performance assessment is required.

Finally, the number of borehole heat exchangers has a direct impact on system performance. With only three boreholes, the Darmstadt system has a limited thermal interaction volume. Scaling up the borehole field would improve both the storage capacity and the consistency of the thermal response and is a necessary step toward achieving recovery efficiencies corresponding with the heat injection volumes (Figure 10).

4. Delft site

The Delft demonstration site focuses on the integration of high-temperature aquifer thermal energy storage (HT-ATES) into the geothermal-based heating system of the TU Delft campus and the connected Delft city district heating network [10]. The system is schematically represented in Figure 11, and designed to store surplus heat from the geothermal source during periods of low heat demand and to recover this heat when demand exceeds the available geothermal supply. In this configuration, the HT-ATES acts as a seasonal buffer between heat production and heat demand, supporting a more flexible and renewable heat supply. The co-simulation work for Delft couples a DARTS-based subsurface model with a TESPy-based surface energy system model to evaluate the interaction between storage behaviour, system operation and heat demand over multiple years.

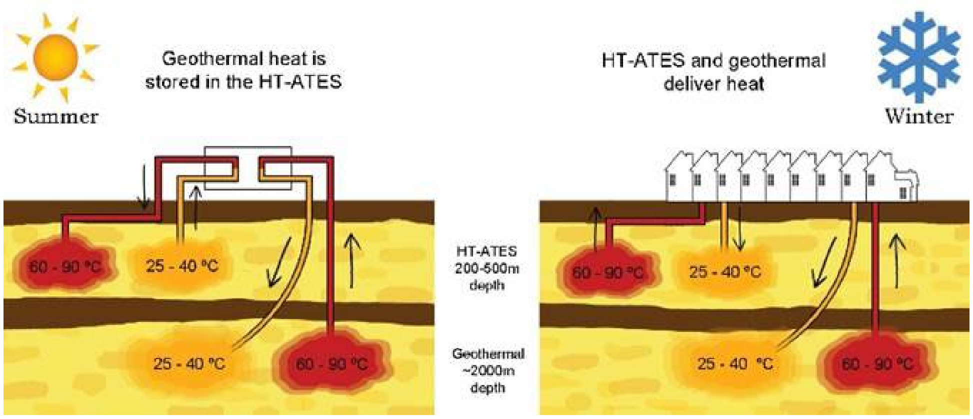

Figure 11: General working principle of geothermal and ATES in conjunction in Delft site [3]

4.1. Goals of Co-Simulation

The objective of the Delft co-simulation is to provide practical insights into the long-term integration of HT-ATES with the surface energy system by analysing how temperature evolution, energy flows and operational decisions affect system utilisation. By explicitly coupling a surface model with a subsurface model, the co-simulation framework captures dynamic interactions that would be overlooked in standalone simulations. This enables a detailed assessment of the system's evolution under realistic operating conditions, including the long-term development of well temperatures, the contribution of different heat sources over time and the role of control strategies such as dynamic cutoff logic.

The results are intended to support the design and operation of future HT-ATES systems, particularly in large-scale district heating networks where fluctuating demand, weather conditions and operational uncertainty require integrated evaluation to identify suitable design and control strategies.

4.2. Simulation scenarios

The Delft co-simulation scenarios were designed to evaluate the seasonal operation of the HT-ATES system as part of the geothermal-based heating network of the TU Delft campus (TUD) and the connected Delft city district heating grid (OWD, Open Warmtenet Delft). The scenarios focus on how the system switches between direct geothermal heat supply, HT-ATES charging, HT-ATES discharging and auxiliary heat supply under varying heat demand conditions.

The main simulation was carried out over a 10-year period in order to capture the long-term development of the storage system over multiple seasonal cycles. Heat demand was represented by a sinusoidal demand profile fitted to measured hourly heat demand data from the TU Delft campus, as shown in Figure 12. The methodology used to construct this profile follows the approach previously detailed by Akin and Daniilidis (2025) [11], where measured consumption data were processed and fitted to a smooth sinusoidal function to enable consistent and repeatable simulation. This approach captures the main seasonal characteristics of building heat demand while reducing short-term fluctuations that are less relevant for annual-scale assessment.

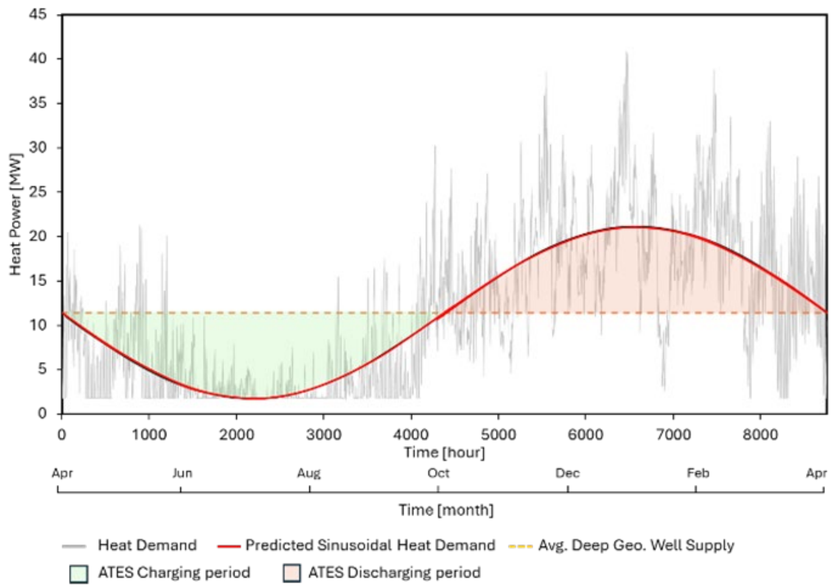

Figure 12: Annual sinusoidal demand profile fitted to measured hourly campus data [12]

During periods of low heat demand, excess geothermal heat is available and the HT-ATES system operates in charging mode. In this mode, geothermal heat is supplied to the network where required, while the remaining surplus heat is directed to the HT-ATES hot well for seasonal storage. During periods of higher heat demand, the system can operate in discharging mode. Stored heat is then extracted from the HT-ATES and supplied to the heating network, potentially with temperature upgrading through the heat pump and with additional support from the boiler when required. A third operational state is bypass or rest mode, in which the HT-ATES is not actively used and heat demand is met directly by geothermal supply and, if necessary, auxiliary heat sources.

The active operational mode is selected dynamically at each timestep based on heat demand, available geothermal heat, temperature levels and storage availability. This setup allows the scenario analysis to represent not only seasonal charging and discharging, but also the feedback between surface operation and subsurface temperature development. The detailed representation of the subsurface model, the surface energy system and the data exchange between both models is described in the following sections.

The simulation was initiated during the charging season. This allows the storage, initially at ambient subsurface temperature, to receive surplus geothermal heat before the first discharge period. This starting condition is important because the early years of operation are affected by the initial thermal state of the storage volume. Therefore, the 10-year simulation horizon was selected to distinguish initial heating-up effects from the more representative long-term seasonal behaviour of the integrated system.

4.3. Underground model setup

The underground component of the Delft co-simulation was developed using the Delft Advanced Research Terra Simulator (DARTS), an open-source reservoir simulation framework developed at TU Delft [3].The model provides a spatially resolved representation of the HT-ATES reservoir and is used to simulate coupled thermal and hydraulic processes in the aquifer over multiple seasonal charging and discharging cycles [12], [13]. This allows the underground model to evaluate thermal plume development, well temperature evolution and the long-term subsurface response of the storage system.

The model represents the subsurface domain of the TU Delft HT-ATES system in three dimensions, as presented in Figure 13. The target storage aquifer is located in the Maassluis Formation, between approximately 130 and 190 m depth. The model domain covers 1,500 m by 1,500 m laterally and extends 500 m vertically. A refined horizontal grid resolution of 5 m is applied around the wells to capture the steep thermal and hydraulic gradients near the injection and production points, while coarser grid spacing is used toward the model boundaries to reduce computational cost. In the vertical direction, variable grid resolution is used to represent the stratified nature of the subsurface, particularly across low-permeability layers [13].

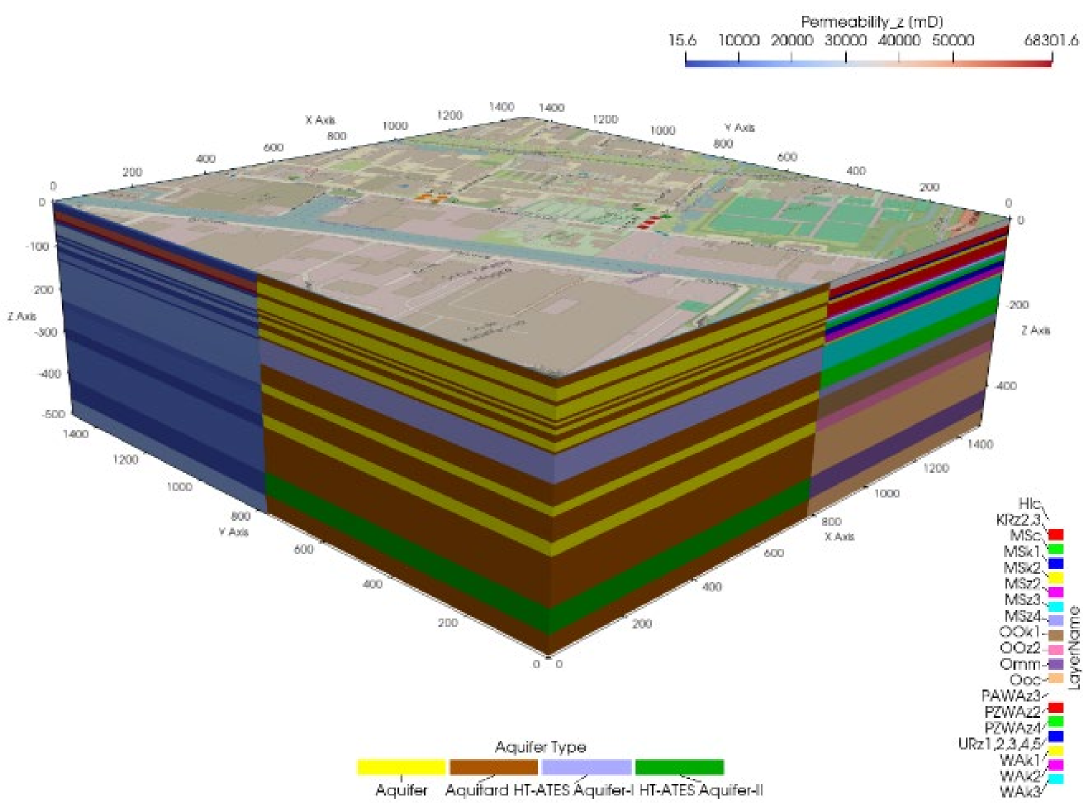

Figure 13. The 3D geological model of the TU Delft campus subsurface, illustrating the distribution of aquifers and aquitards (middle part), permeability variations (left), and formation names (right) [13]

Boundary conditions are defined to represent the larger hydrogeological setting around the storage system. Dirichlet-type lateral boundary conditions are used to maintain representative hydraulic head and temperature gradients at the model edges, while the top and bottom boundaries are closed to flow and heat. The simulations are performed using the operator-based linearisation framework implemented in DARTS, which improves computational efficiency by replacing nonlinear terms with multidimensional interpolation tables. This enables stable simulation of coupled thermal and hydraulic processes under heterogeneous subsurface conditions [3], [14].

Within the co-simulation, the DARTS model receives well operation data from the surface energy model at each timestep. In charging mode, the temperature and flow rate of the water returning to the hot well are passed to DARTS. In discharging mode, the reinjection temperature and flow rate toward the warm well are provided. Based on these inputs, DARTS computes the subsurface response for the timestep by solving for pressure and enthalpy across the 3D reservoir domain. The relevant production or injection temperatures are then retrieved from the well domain and returned to the surface model for the next timestep [12].

4.4. Surface components model setup

The surface energy system of the Delft co-simulation was modelled using the Thermal Engineering Systems in Python (TESPy) framework. TESPy is a component-based modelling tool for thermal engineering systems and solves the thermodynamic state of connected components by applying mass and energy balances across the network [7]. In the Delft model, TESPy is used to represent the above-ground energy infrastructure and to calculate the pressure, temperature, enthalpy and mass flow conditions throughout the surface system at each timestep.

The modelled surface system includes the deep geothermal doublet, heat exchangers, a heat pump, the HT-ATES interface, auxiliary heat supply and the heat delivery paths to the TUD and the connected Delft city district heating grid (OWD). The geothermal doublet provides heat at approximately 75-80 °C. Depending on the heat demand and the required temperature level, this geothermal heat can be supplied directly to the heating network, used in combination with the heat pump, or partly directed to the HT-ATES system for seasonal storage during periods of surplus geothermal production.

The TESPy network is built from interconnected thermal components that represent the main heat transfer and flow paths in the system. Heat exchangers are used to transfer heat between the geothermal source, the district heating side and the HT-ATES interface. The heat pump is included to upgrade the temperature level when stored or available heat is not sufficient to meet the required supply conditions. Auxiliary heat supply is represented to cover demand that cannot be met by the geothermal source and HT-ATES system alone. The model therefore captures the main surface-side interactions between heat production, heat storage and heat demand.

The surface model can be configured for three operational states: ATES charging, ATES discharging and ATES rest. These configurations are shown in Figure 14. In the charging configuration, surplus geothermal heat is stored to the HT-ATES hot well. In the discharging configuration, stored heat is recovered from the HT-ATES and supplied to the heating network, with temperature upgrading where required. In the rest configuration, the HT-ATES is bypassed and heat is supplied directly from the geothermal source and auxiliary units where needed. These configurations define the possible flow paths represented in TESPy, while the broader operational implications are discussed in the simulation results and discussion sections.

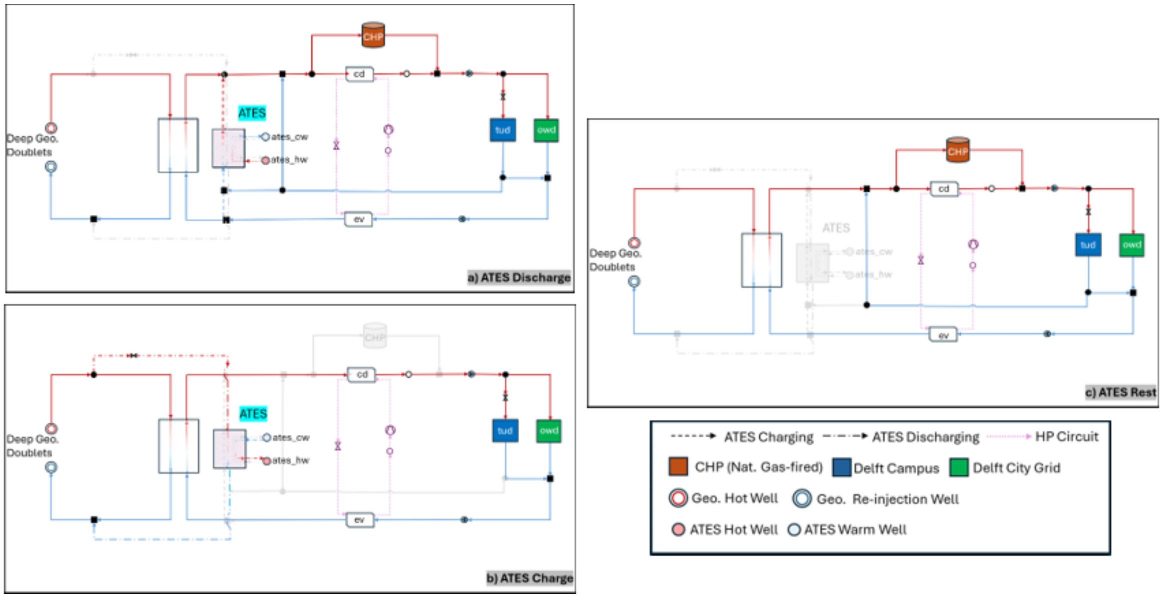

Figure 14. TESPy configuration for each operation mode: (a) ATES Discharging, (b) ATES Charging, (c) ATES Rest

For each timestep, TESPy calculates the thermodynamic state of the active surface system configuration. The relevant outputs include component heat duties, connection temperatures, mass flow rates and energy flows. At the HT-ATES interface, the surface model provides the temperature and flow rate conditions required by the DARTS subsurface model. In return, updated well temperatures from DARTS are used in the next surface model calculation. In this way, TESPy represents the surface-side response of the integrated system while DARTS represents the underground storage behaviour.

4.5. Simulation results

This section presents the simulation results obtained from the integrated TESPy and DARTS co-simulation framework for the Delft site. Over the 10-year period, the evolution of subsurface temperatures, surface component interactions and overall heat supply were analysed to assess the system performance.

4.5.1. Thermal stabilisation of ATES wells

The first result concerns the thermal stabilisation of the ATES wells. The simulated temperature development of the hot and warm wells over the simulation period is shown in Figure 15. In the early years of operation, both hot and warm wells show seasonal variations as the reservoir adjusts from initial ambient ground temperature of approximately 12 °C. The hot well temperature rises rapidly during charging periods due to the injection of surplus geothermal heat, reaching values close to the geothermal supply temperature of around 75 °C. The warm well, which acts as the production well during charging and as the injection well during discharging, shows larger temperature variations in the early years and drops to near 20 °C during early discharge cycles.

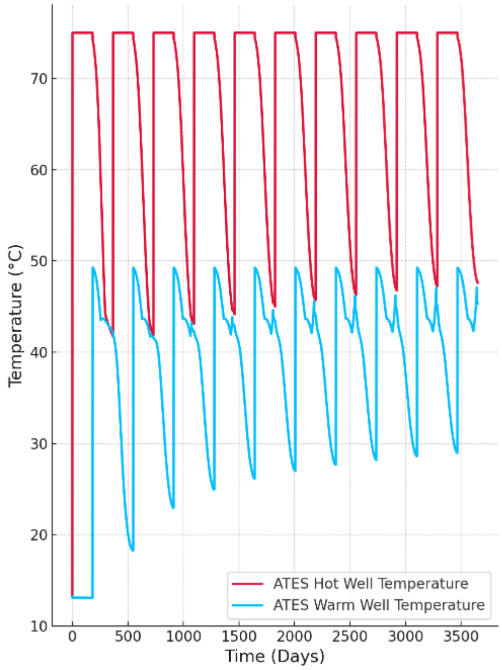

Figure 15: Temperature development of the hot and warm wells over the 10-year simulation period

By the year six, the system operation begins to stabilise in performance. The hot well temperature converges fluctuating between approximately 45 °C and 75 °C with reduced year-on-year variation. Similarly, the warm well temperature settles into a cyclic band between approximately 27°C and 49°C.

4.5.2. Energy flows and source contributions

The evolution of well temperatures also affects the distribution of heat supply from different sources. Figure 16 shows the heat power distribution by source in the first and tenth operational years. In the first year, a significant share of the geothermal energy is directed to charging the ATES wells during the low-demand period. This reflects the initial heating up of the cold subsurface environment. In the same early period, the contribution of ATES to direct heating is relatively limited and the auxiliary boiler contribution is more visible during peak demand periods. By the tenth year, the distribution shifts. The need for this initial heating up decreases as the ATES wells stabilise thermally, allowing a larger share of geothermal output to be used directly to meet the heat demand. ATES discharging becomes more dominant and consistent, while CHP and boiler contribution is reduced.

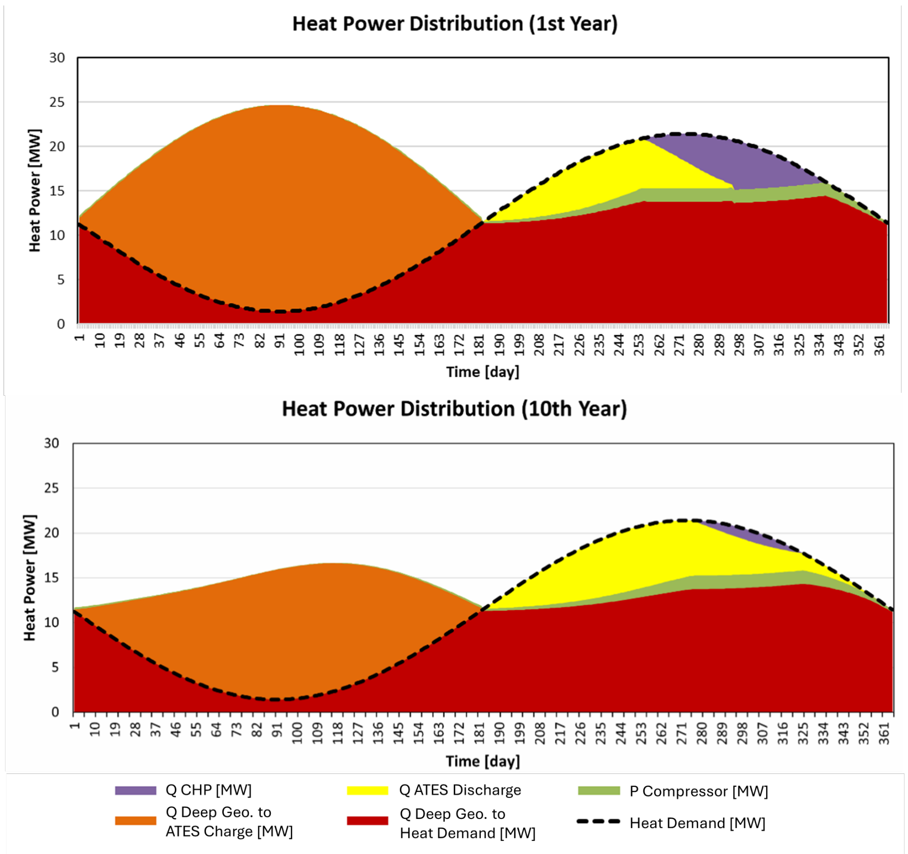

Figure 16: Heat power distribution by source in the first and tenth operational years

The annual energy distribution from the geothermal production to ATES charging and direct heat supply is shown in Figure 17. In the first year, the total energy extracted from the deep geothermal doublet is approximately 6,024 MWh. Around 45.5% of this energy is directed to charging the ATES wells, while 54.5% is used to supply heat demand. Over the following years, the share of geothermal energy directed to ATES charging decreases to approximately 34.5%, while the share delivered directly to the network increases to nearly 65.5%. The renewable energy share also improves over time and exceeds 95% by the end of tenth year.

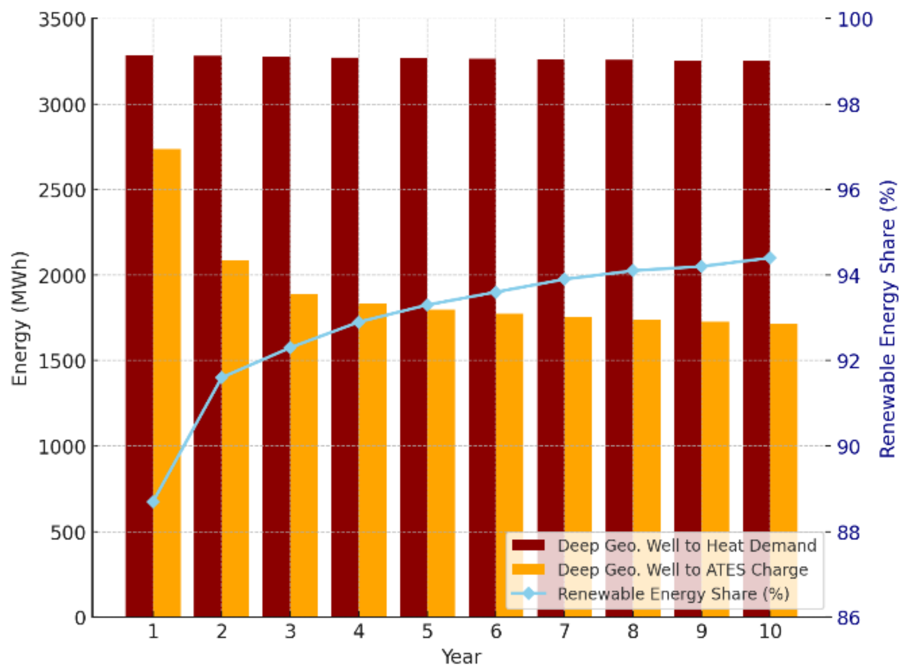

Figure 17: Annual energy distribution from geothermal production to ATES charging and direct heat supply, with renewable energy share shown on the secondary axis

4.5.3. Heat demand coverage

The yearly heat demand contribution by source is shown in Figure 18. The geothermal supply remains the primary and baseload source, maintaining a relatively consistent annual out of around 3260 MWh. At the start of the operation, the ATES contribution is relatively low because the warm well requires time to thermally stabilize. Over time, ATES contribution to heat supply increases steadily and reaches around 680 MWh in year 10. At the same time, the boiler contribution decreases from approximately 258 MWh in year one to 39 MWh by year ten.

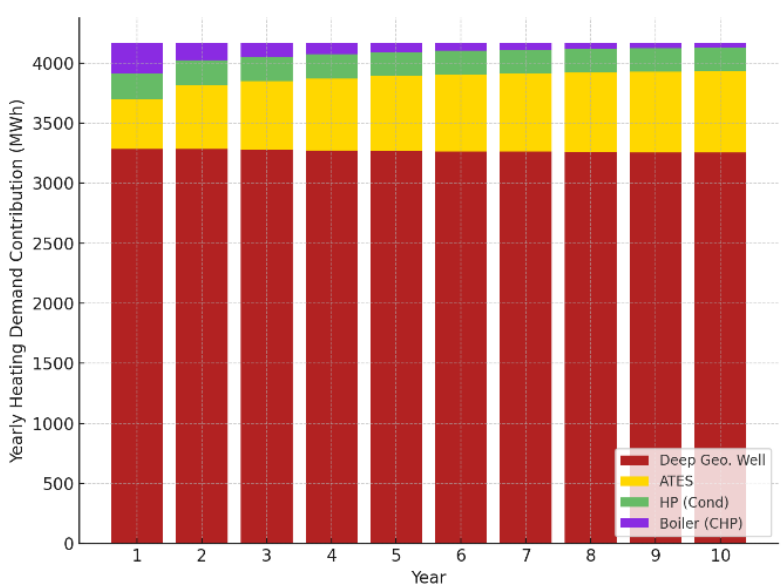

Figure 18: Yearly heating demand contribution by heat source

4.5.4. Dynamic cut-off control

The co-simulation also evaluates the effect of a dynamic cut-off strategy on ATES operation. The cut-off logic determines whether ATES discharge is feasible by comparing the return temperature from the city grid*, T_ret*, with the available temperature at the ATES hot well, *T_hw.* If the thermal gradient is sufficient with the margin, defined as *T_hw > T_ret + 2°C*, the system proceeds to discharge mode. Otherwise, it picks the rest mode to prevent inefficient heat extraction. The annual distribution of charge, discharge and rest days is shown in Figure 19. Over the simulation, the number of ATES hot well rest days decreases, while the number of discharge days increases. This shift follows the rising aquifer temperature at the ATES site and the application of the cut-off based operating logic.

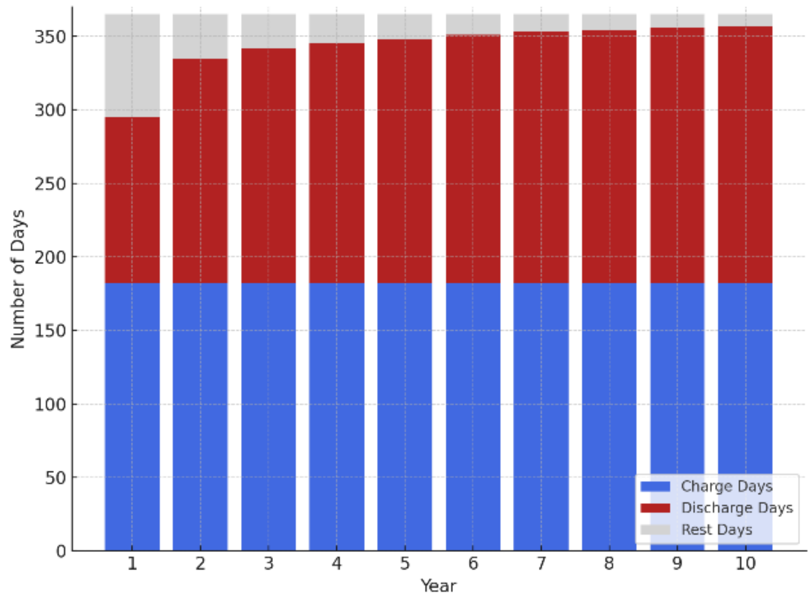

Figure 19: Annual distribution of operational days in charge, discharge and rest modes for ATES

4.5.5. Upscaled implementation

Whereas the upscaling analyses at Darmstadt and Bochum address the storage itself, at Delft the storage is not the binding element of the current design: the heat pump centre is dimensioned at the capacity of the geothermal well, with an evaporator throughput of 400 m³/h against a condenser capacity of 770 m³/h. During discharge, the ATES flow can therefore only be delivered directly to the network while its supply temperature exceeds the network return. Routing through the heat pump evaporator is not possible as long as the geothermal well operates at nominal flow. An increase of the heat pump capacity to further accommodate the HT-ATES has been identified as a possible development option for the site. Three upscaling scenarios are therefore examined.

1. The first quantifies this option by enlarging the evaporator to the combined nominal flow of the geothermal well and the ATES (670 m³/h), leaving the wells, the ATES design flow, and the condenser unchanged.

The second and third scenarios address the balance between source, storage and demand:

2. a supply-rich (Geo-rich) configuration, in which the geothermal supply is increased by 50 % with the evaporator enlarged by the same sizing rule,
3. and a demand-rich configuration, in which the heat demand is increased by 50 % instead.

Together, the three scenarios examine which element of the integrated system limits the utilisation of the storage. The scenarios were simulated using a standalone Modelica model of the Delft system developed within Task 3.2, where it serves as the virtual demonstration environment for the smart-controller development. The model represents the geothermal supply, central heat pump, the OWD and TUD demand connections and the ATES doublet using the "MultiWell" model of the Modelica Buildings Library, with a supervisory controller selecting between charging and four discharge configurations. Analogous to the standalone bore field comparison at the Darmstadt site (Section 4.5.4), this lower-order representation complements the spatially resolved DARTS–TESPy co-simulation and illustrates the range of model fidelities employed within the project.

Scenario 1 – upscaled evaporator

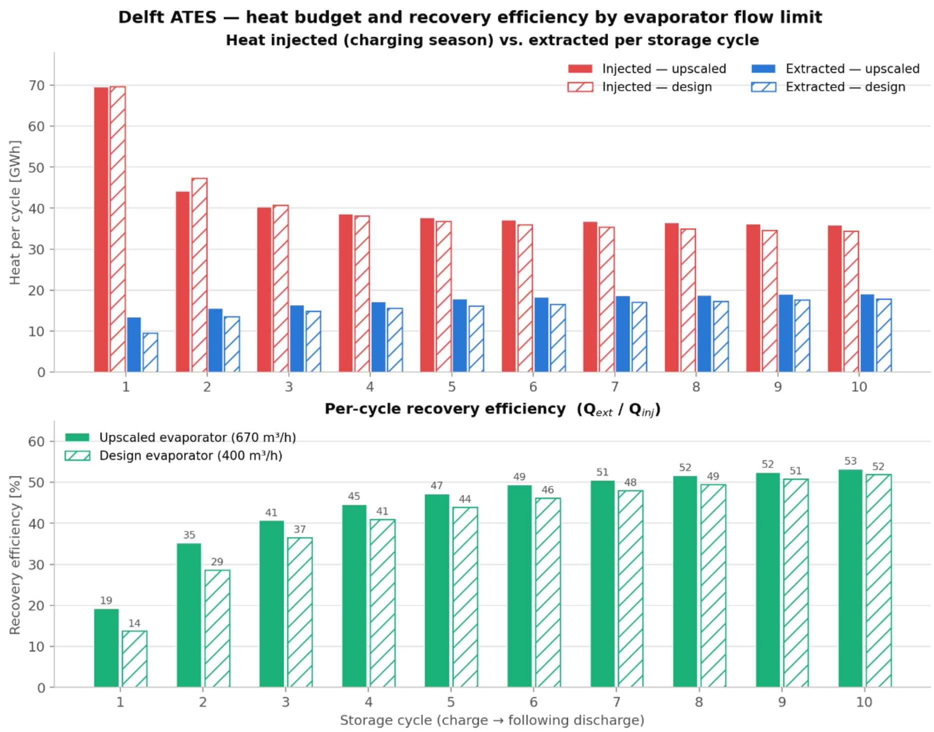

Figure 20: Comparison of the design and the upscaled implementation of the heat pump and ATES system

Figure 20 compares the heat budget and recovery efficiency per cycle of the two configurations over ten complete storage cycles. One cycle consists of a charging season followed by a discharge season. Over ten cycles, the enlarged evaporator increases total heat extraction from 155.9 GWh to 173.8 GWh with almost no change in injection, resulting in an increase in overall recovery efficiency from 38.2% to 42.1%. However, the benefit is concentrated in the early cycles. The first-cycle recovery rises from 13.7% to 19.2%, whereas by the tenth cycle, the configurations differ by little more than one percentage point (51.9% versus 53.2%). This behaviour follows directly from the operating modes. With the standard evaporator design, the ATES discharge is effectively restricted to direct delivery. This requires the hot-well supply temperature to exceed the network return temperature, meaning that each discharge season terminates once the storage falls below this threshold and the remaining lower-grade heat is lost. In contrast, the enlarged evaporator allows the ATES flow to be routed through the heat pump evaporator alongside the geothermal stream. This extends extraction into the low-temperature tail of each season. As the storage warms over successive cycles and the direct-delivery window lengthens, the two configurations converge. Therefore, evaporator capacity primarily governs the speed with which the integrated system approaches its optimal performance and the extent of heat recovery during the transient phase, which can span multiple years. It does not directly impact equilibrium recovery efficiency.

Scenario 2 & 3 – upscaled geothermal supply and demands

Figure 21 to Figure 24 compare the supply-rich and demand-rich configurations over ten simulated years. The two scenarios behave in fundamentally different ways, and in each case a different element limits the use of the storage.

Figure 21 shows the heat delivered over the ten-year period by source. In the supply-rich configuration the system delivers around 3,600 TJ in total, of which 2,903 TJ come from the geothermal source via the heat pump, 368 TJ from the ATES and only 329 TJ from the gas boiler. In the demand-rich configuration the total delivery rises to around 5,400 TJ. The geothermal contribution increases to 3,744 TJ and the ATES contribution to 469 TJ, but the gas boiler must cover 1,187 TJ of the demand that geothermal supply and storage cannot meet. The supply-rich system therefore operates nearly gas-free, yet is likely to have additional capital intensive installations, while the demand-rich system remains substantially dependent on the auxiliary boiler, with a low (comparatively) capital investment.

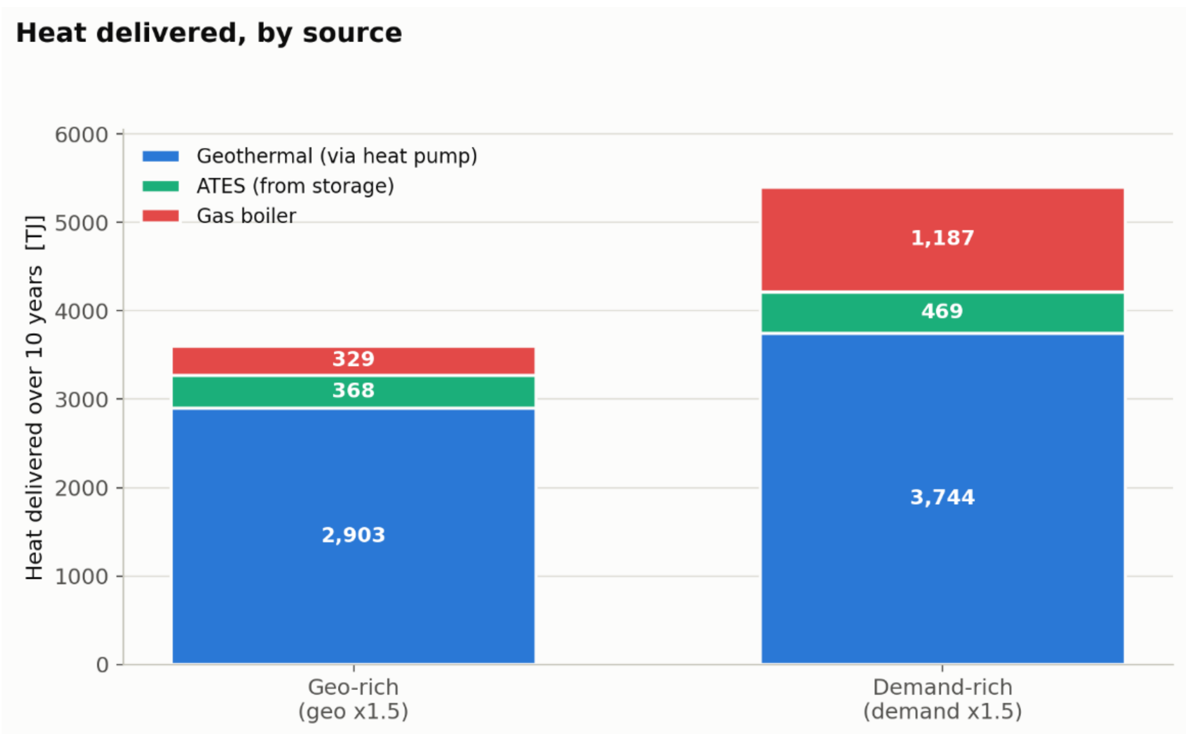

Figure 21: Comparison of the delivered heat of the different sources for upscaled demands and geothermal supplies.

Figure 22 shows the development of the ATES recovery efficiency. In the supply-rich case the efficiency plateaus early and reaches only 22 % by year ten. This does not indicate poor storage performance but reflects that the residual demand for stored heat is small compared to the amount injected. In the demand-rich case the recovery efficiency climbs continuously and reaches 50 % by year ten.

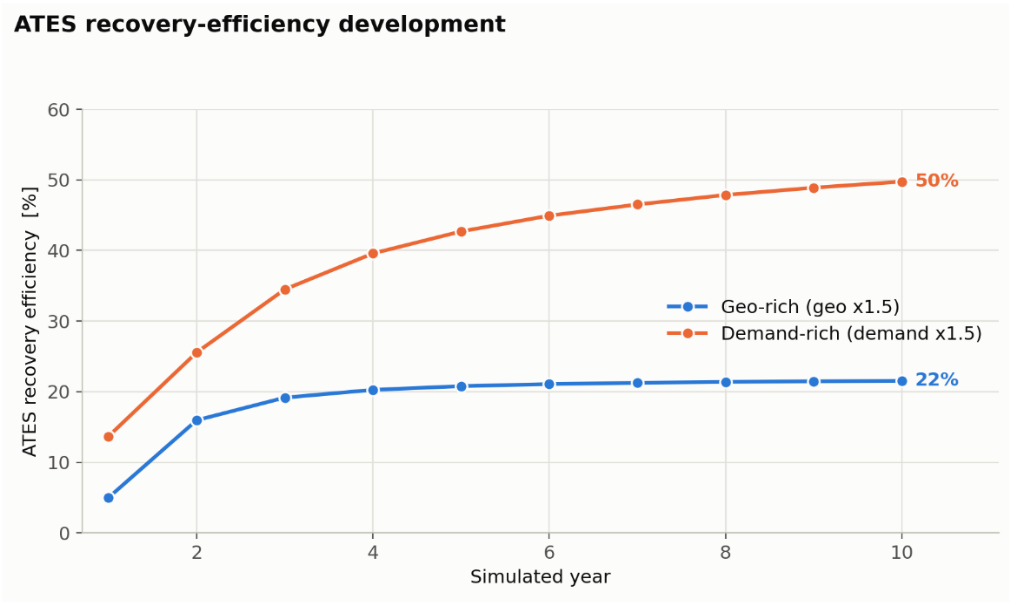

Figure 22: Development of the storage recovery efficiency over the 10-year simulation time

In Figure 23, the annual energy charged into and discharged from the ATES is shown and it explains this behaviour. In the supply-rich configuration the surplus geothermal heat allows the storage to be charged at approximately 190 to 200 TJ per year after the first cold-start cycle, while the discharge is limited by the residual demand and settles at approximately 41 TJ per year. The demand, not the available energy, limits the use of the ATES. In the demand-rich configuration the situation inverts. The higher direct use of geothermal heat leaves less surplus for charging, which declines from 220 TJ in the first year to approximately 105 TJ per year, while the discharge rises to approximately 52 TJ per year. Here the available charging energy limits the ATES, which also explains the high recovery efficiency observed in Figure 22 and Figure 23.

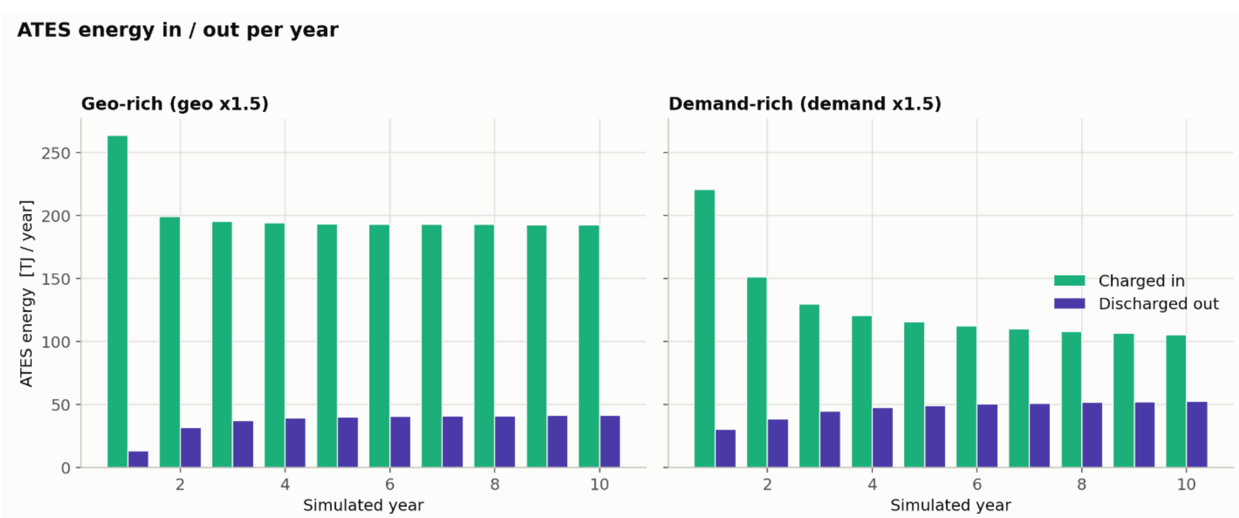

Figure 23: Yearly charged and discharged energy of the ATES for the two scenarios

In the supply-rich configuration the capacity factor settles at 34 % and only 35 % of the produced geothermal energy is harvested for direct use or ATES charging, with the remainder reinjected warm. In the demand-rich configuration the capacity factor reaches 47 % and 50 % of the produced energy is harvested. The larger demand thus makes considerably better use of the geothermal source, at the cost of the additional gas consumption shown in Figure 21.

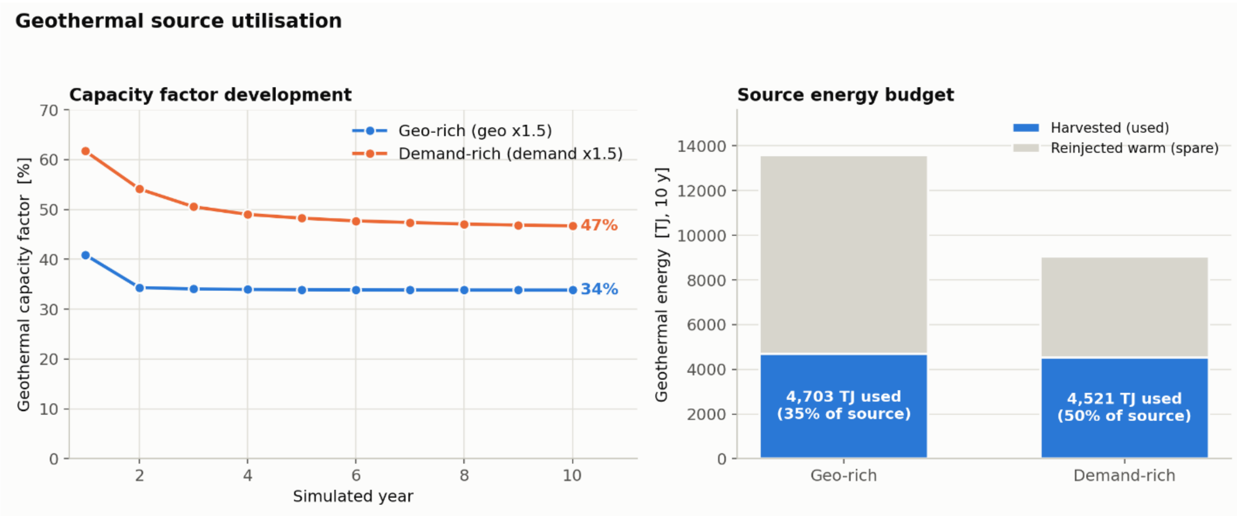

Figure 24: Heat budget and utilisation of the geothermal source for the two scenarios

The comparison illustrates that recovery efficiency alone is a misleading performance indicator. The demand-rich case achieves more than twice the recovery efficiency of the supply-rich case while emitting substantially more CO_2eq, echoing the observation at the Bochum site that the system-level metric matters more than the component-level one. It should be noted that the supply-rich case will probably have a higher capital investment (which is not the focus of this work). Good performance requires the geothermal supply, the storage capacity and the heat demand to be mutually tuned. The storage enables efficient use of the geothermal source only where the demand exists to absorb the recovered heat.

4.6. Discussion

The results show that the performance of the integrated HT-ATES and surface heating system changes over multiple seasonal cycles. The first years of operation are strongly influenced by the initial ambient temperature of the reservoir. During this period, part of the geothermal energy is used to increase the temperature of the ATES wells and surrounding aquifer, As a result, the ATES contribution to heat supply is lower in the early years and auxiliary boiler support is more visible during peak demand periods.

As wells stabilise thermally, the contribution of the ATES system becomes more consistent. The reduction in the share of geothermal heat is directed to ATES charging, from 45.5% to 34.5% and the corresponding increase in direct geothermal heat supply, from 54.5% to 65.5%, indicate that less energy is required to bring the storage system to be operational temperatures. The increase in ATES discharge and decrease in boiler contribution also show that the integrated system gradually shifts toward greater use of stored geothermal heat in ATES.

The behaviour is closely linked to the concept of bridging energy. In the early years, the initially cold storage volume requires additional geothermal energy before it can contribute more effectively during discharge periods. As the warm well temperature increases over the cycles, less energy needed to prepare the storage for operation, and ATES discharging becomes more dominant and consistent. This explains the gradual increase in stored heat utilisation and the reduction in auxiliary boiler contribution.

The dynamic cut-off control strategy shows how the surface system can respond to the evolving thermal state of the subsurface. In this strategy, ATES discharge is only activated when the hot well temperature is sufficiently above the return temperature from the heating network. If the condition is not met, the ATES system remains in rest mode to avoid inefficient discharge. Over the 10-year simulation, the number of rest days decreases and the number of discharge days increases following the gradual thermal stabilisation of ATES wells.

The results demonstrate the added value of the co-simulation framework. TESPy represents the surface energy system, including heat demand, component operation and surface facilities, while DARTS represents the subsurface temperature and storage behaviour. The interaction between these two domains determines the long-term evolution of well temperatures, energy flows and operational modes. This interaction would not be represented in the same way by standalone surface or subsurface simulations.

The interpretation of the results should consider the assumptions of the current model setup. The heat demand is represented by a sinusoidal profile fitted to measured campus data, which is suitable for long-term seasonal analysis but does not capture all short-term demand variations. The deep geothermal source is represented with a constant thermal output. The return temperature from the heating network is dynamically computed and used in the system operation, but the effect of this variable reinjection temperature on geothermal production performance is not explicitly modelled. The results should therefore be interpreted as a system-level assessment of HT-ATES integration under the defined scenario assumptions.

4.7. Lessons learnt

The Delft co-simulation provides the following lessons for the design and operation of HT-ATES systems integrated with district heating networks:

- The use of ATES substantially increases the renewable energy share of heat supplied, with the share increasing rapidly over the first few years of operation.
- The amount of energy recovered from the HT-ATES is a considerable proportion of the energy injected.
- Thermal stabilisation of the ATES wells occurs gradually over multiple seasonal cycles. The first years of operation are affected by the initial ambient temperature of the storage volume. Long-term simulation is therefore needed to evaluate representative system behaviour
- The early years require bridging energy. A significant part of the geothermal energy is initially used to heat up the storage system and bring it toward its operational temperature range. This affects the early balance between ATES charging, direct geothermal heat supply and auxiliary boiler use. This is likely to be at the same time when heat demand is growing.
- Source contributions change over time. As the ATES wells stabilise thermally, a larger share of geothermal heat can be supplied directly to the network, while ATES discharging becomes more consistent. This leads to a gradual reduction in the contribution of auxiliary boiler support.

- Dynamic cut-off control improves operational responsiveness. By activating ATES discharge only when the hot well temperature is sufficiently above the network return temperature, the system avoids inefficient operation and makes better use of stored heat.
- Co-simulation is needed to capture the interaction between the surface system and the subsurface reservoir. The Delft case shows that heat demand, component operation, well temperature development and storage availability evolve together over time. Coupling TESPy and DARTS allows these interactions to be represented.
- Enlarging the evaporator to the combined well and ATES flow raises first-cycle recovery from 13.7 % to 19.2 % and cumulative ten-year extraction by approximately 12 %, while the equilibrium recovery efficiency remains nearly unchanged.
- Recovery efficiency alone is a misleading performance indicator. The supply-rich scenario reaches only 22 % recovery efficiency yet operates nearly gas-free, while the demand-rich scenario reaches 50 % but requires more than three times the gas-boiler energy. The balance between geothermal supply, storage capacity and heat demand determines system performance, and the storage only enables efficient use of the geothermal source where sufficient demand exists to absorb the recovered heat.

5. Bochum site

The Bochum demonstration site addresses mine thermal energy storage (MTES), the third of the three storage technologies investigated within PUSH-IT. The site is located at the technical centre (Technisches Zentrum) of the Ruhr-University Bochum (RUB), where the storage volume is formed by abandoned, water-filled mine galleries of the former Mansfeld colliery and is to be connected to the university's existing district heating and cooling infrastructure. This network supplies not only the RUB campus but also extends into the surrounding districts. The energy system is operated through a joint venture between the university and Stadtwerke Bochum. Heat is currently generated centrally at the technical centre by two combined heat and power (CHP) units, supported by gas-fired boilers that cover peak loads, while cooling is provided by three turbo chillers supported by cooling towers. An arial overview of the heat generation facilities and the location of the used mine for storage is provided in Figure 25.

The co-simulation work for the Bochum site couples a low-order, physics-based MTES model implemented in Python with a Modelica model of the surface energy system, exchanging boundary conditions through a Python orchestration layer into which the Modelica model is integrated as a Functional Mock-up Unit (FMU). The work follows the consistent structure used for the other demonstration sites: goals, scenarios, the underground and surface model setups, results, discussion, and the transferable lessons learned.

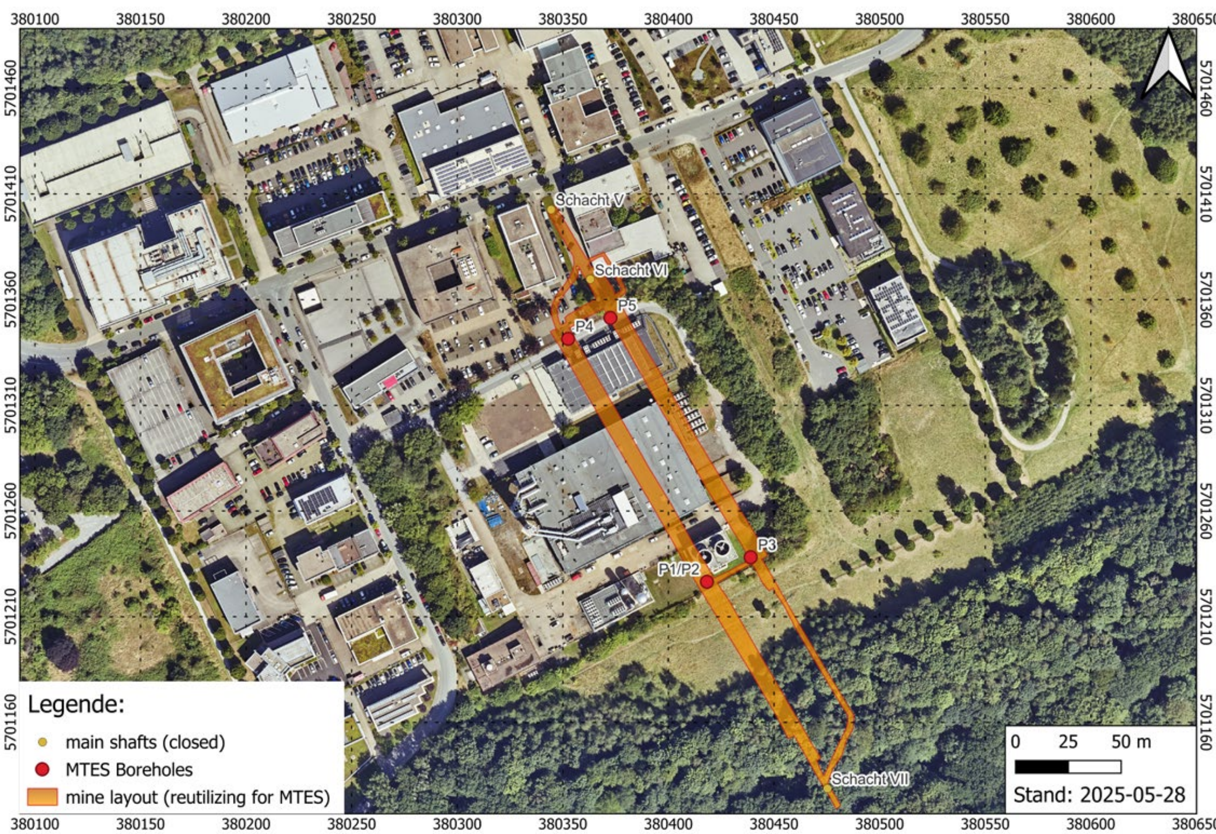

Figure 25: Satellite view of the two mine galleries of the former Mansfeld colliery used as the MTES volume, together with the planned boreholes and the location of the technical centre relative to the RUB campus

5.1. Goals of Co-Simulation

The overarching goal of the Bochum co-simulation is to assess whether mine thermal energy storage can be integrated into the existing heating and cooling system of the Ruhr-University Bochum and, if so, to quantify the technical, environmental, and techno-economic performance of the resulting integrated system.

The motivation for the new system is rooted in the operation of the present configuration. Today, waste heat from the cooling cycle is rejected to the atmosphere through the cooling towers, while peak heating load is met by gas boilers. The fundamental idea of the proposed system is to recover this waste heat and use it in the heating cycle, thereby reducing both cooling-tower and gas-boiler operation, with the longer-term ambition of phasing out both entirely. A heat pump is placed between the turbo chillers and the cooling tower so that the condenser-side output of the chillers becomes the evaporator-side input of the heat pump, upgrading the waste heat for use in the heating cycle. Because the cooling demand is relatively continuous throughout the year, this heat pump can provide a steady base load to the heating cycle alongside the CHP units. When there is no immediate heating demand, or when waste heat is available in excess, the MTES stores the surplus thermal energy for later use, thereby addressing the seasonal mismatch between heat supply and demand that motivates seasonal storage in the first place.

In the co-simulation framework, the MTES therefore acts as an efficient thermal link between the waste-heat source on the cooling side and the heating demand. The specific objectives of the Bochum co-simulation are: to evaluate the temperature behaviour of the storage volume and the surrounding rock over seasonal cycles; to quantify the technical performance of the new components, expressed through the system coefficient of performance (COP) and the achievable reduction in gas-boiler and cooling-tower use; to determine the associated annual CO_2 savings; and to assess the levelised cost of heat (LCOH) of the storage system. A further objective is to establish, through sensitivity analysis, how component dimensioning and operational parameters influence these outcomes, and thereby to identify a practical and a theoretical optimum configuration.

5.2. Simulation scenarios

The co-simulation was driven by two-and-a-half years of measured operational data for the RUB heating and cooling network. Data for the years 2022 and 2023 were used consecutively. Because charging the storage during summer (when waste heat is plentiful and heating demand is low) reflects realistic operation, the simulation period was defined to begin at the start of the German summer season on 21 June, combining the data from 21 June to the end of 2022 with the two full years of data. This period was chosen on the basis of data availability and because it represents a realistic timeframe within the PUSH-IT project; for a commercial deployment a longer horizon would be preferable.

The reference, or case-study, scenario uses the standard set of input parameters described in Sections 5.3 and 5.4, with a 2.5 MW heat pump and a storage volume of 7,000 m³. Around this reference, a structured set of scenarios was defined to test the behaviour and robustness of the coupled system:

Component sizing was varied by simulating heat-pump sizes from 1 MW to 7 MW in steps of 1.5 MW, and MTES volumes of 4,000, 7,000, and 10,000 m³, the upper value reflecting the maximum volume considered feasible within the available mine. Each combination of heat-pump and storage size was also simulated to examine how the two interact. Operational parameters were varied by testing the minimum temperature difference imposed across the heat pumps (ΔT) over the range 0 K to 15 K in steps of 5 K, and the maximum MTES operating temperature at 40, 50, 60, and 70 °C; again, all combinations were simulated. To test robustness against demand variability, a "cold years" scenario (heating demand increased by 10 % and cooling demand decreased by 10 %) and a "hot years" scenario (the inverse adjustment) were defined. Finally, a long-term scenario was constructed by looping the two-year dataset over 20.5 years to identify when the storage reaches a quasi-steady thermal equilibrium. The scenario set culminates in two optimal configurations, one constrained to physically realisable parameters (the practical optimum) and one in which the storage volume is sized to the theoretical optimum without regard to the boundaries of the existing mine.

5.3. Underground model setup

The defining methodological characteristic of the Bochum site is the representation of the storage volume by a low-order, physics-based model implemented in Python rather than by a spatially resolved three-dimensional numerical model. This is a deliberate and well-justified modelling choice. The storage volume consists of abandoned mine galleries whose geometry, hydraulic connectivity, and thermal properties are only partially known. Constructing a high-fidelity finite-element model on the basis of such uncertain geometry and poorly constrained parameters would impart a false sense of precision without a corresponding gain in predictive reliability. A reduced-order energy-balance model is instead commensurate with the available site knowledge and is well suited to the exploratory aim of the Bochum co-simulation, which is to characterise system behaviour and sensitivity. The Python implementation also offers a particularly direct and transparent coupling, since the storage model and the orchestration logic coexist within a single environment and exchange data through direct function calls. Hence, sophisticated simulation models can be integrated once they have been developed on the basis of real measurement data.

The model captures the energetic interaction between the mine water and the surrounding rock. To make this tractable, the two connected galleries are treated as hydraulically and thermally connected and are simplified to a single underground volume, which is in turn idealised as a cylinder whose volume equals the combined volume of the two chambers and whose length equals their average length. The surrounding rock is treated as homogeneous, disregarding individual coal seams and supporting structures, and the only heat exchange considered between the storage and its surroundings is conduction into the rock.

The storage volume is treated as a fully mixed volume, in which incoming water is assumed to mix immediately with the existing contents and stratification is neglected. This assumption was justified on two grounds. First, the turnover time of the storage, the time required to exchange the full volume once at the design flow rate, is approximately 46 hours for a 7,000 m^3 volume and a flow rate of 150 $m^3\ h^{-1}$, which is short relative to the weeks-to-months duration of a seasonal charging or discharging cycle, so the volume is exchanged many times over a cycle. Second, the Reynolds number at the inlet pipe was evaluated across the relevant range of water temperatures and was found to exceed 10^4 in all cases, well above the turbulent threshold of 4,000, confirming that the inflow is turbulent and therefore well mixed.

The model is built around an energy balance for the storage in which the rate of change of stored energy equals the waste heat entering from the cooling cycle, less the heat withdrawn for the heating cycle, less the conductive exchange with the surrounding rock. The conductive term is derived from Fourier's law applied to the cylindrical surface of the storage and integrated radially between the wall of the storage and the edge of the thermal front, yielding a logarithmic dependence on the ratio of the thermal radius to the storage radius. The storage temperature is advanced over time using this formulation, so that whenever the storage is warmer than the surrounding rock, heat flows outward and the storage cools, and vice versa.

The radial extent of the conductive interaction is governed by the thermal radius, which describes the penetration of heat into the surrounding rock treated as a semi-infinite solid. The thermal radius is approximated as growing with the square root of the product of the rock's thermal diffusivity and elapsed time. Evaluated over a six-month period — the maximum expected duration of a seasonal cycle — the thermal radius reaches approximately 6 m. To handle the fact that charging and discharging produce overlapping warm and cold fronts that are difficult to model directly, a pragmatic and robust simplification was adopted: assuming a maximum charging or discharging cycle of 100 days, a maximum thermal radius is fixed, and the corresponding annulus of rock is treated as a thermal buffer into which heat is conducted during charging and from which heat is conducted during discharging. The governing equation is split into separate updates for the storage and rock temperatures so that the two can evolve individually, with heat transferred from storage to rock during charging and from rock to storage during discharging. A standalone test of this scheme over three 30-day charge/discharge cycles confirmed the expected behaviour, with the rock temperature rising during charging and flattening or declining during discharging.

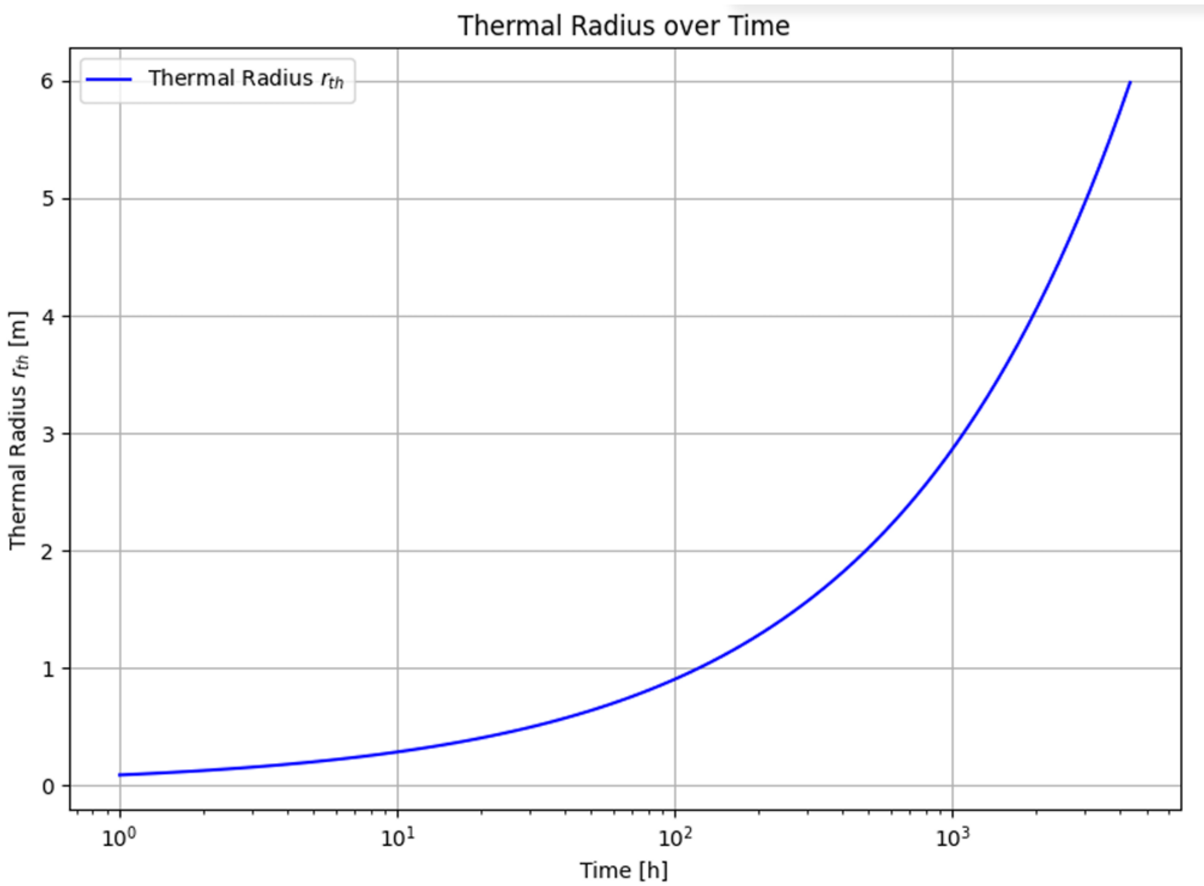

Figure 26: Growth of the thermal radius of the rock surrounding the MTES over time (logarithmic time axis), reaching approximately 6 m after half a year [15]

The physical input parameters comprise rock, water, and storage properties (Table 2). The rock properties were taken from analysis of a nearby borehole at the geothermal centre in Bochum; as the mine lies at a depth of approximately 120 m, sandstone was used, with a thermal conductivity of 3.5 W m^{-1} K^{-1}, a density of 2,469.84 kg m^{-3}, and a specific heat capacity of 1,400 J kg^{-1} K^{-1} (the latter taken as the average of dry and water-saturated sandstone). Water properties were taken as a density of 997 kg m^{-3} and a specific heat capacity of 4,180 J kg^{-1} K^{-1}. The reference storage volume was 7,000 m^3 with an effective length of 178.5 m. The storage was initialised at 11 °C, and its maximum operating temperature was set to 50 °C, the threshold above which storage is regarded as high-temperature, and consistent with the condenser-input temperature of the discharging heat pump, while the minimum operating temperature is determined within the control strategy and depends on heat-pump size (15 °C for the reference 2.5 MW heat pump). The forward Euler method is used to advance the storage state in time.

Table 2: Input parameters of the Python MTES model [15]

Entity	**Parameter**	**Value**	**Unit**
Rock	Thermal conductivity	3.5	W m^{-1} K^{-1}
	Density	2,469.84	kg m^{-3}
	Specific heat capacity	1,400	J kg^{-1} K^{-1}
Water	Density	997	kg m^{-3}
	Specific heat capacity	4,180	J kg^{-1} K^{-1}
Tank	Volume	7,000	m^3
	Length	178.5	m

5.4. Surface components model setup

The surface energy system (Figure 27) was modelled in Modelica using the Dynamic Modelling Laboratory (Dymola) environment, drawing component models from the Modelica Standard Library together with the open-source IBPSA, Buildings, and DisHeatLib libraries. The choice of an equation-based, object-oriented modelling language for the surface side and a procedural language for the storage side reflects the intention to allow either model to be replaced by a different tool at a later stage, the rationale for adopting a co-simulation approach rather than a single monolithic model. The Modelica model represents the heating and cooling system of the RUB and its technical centre.

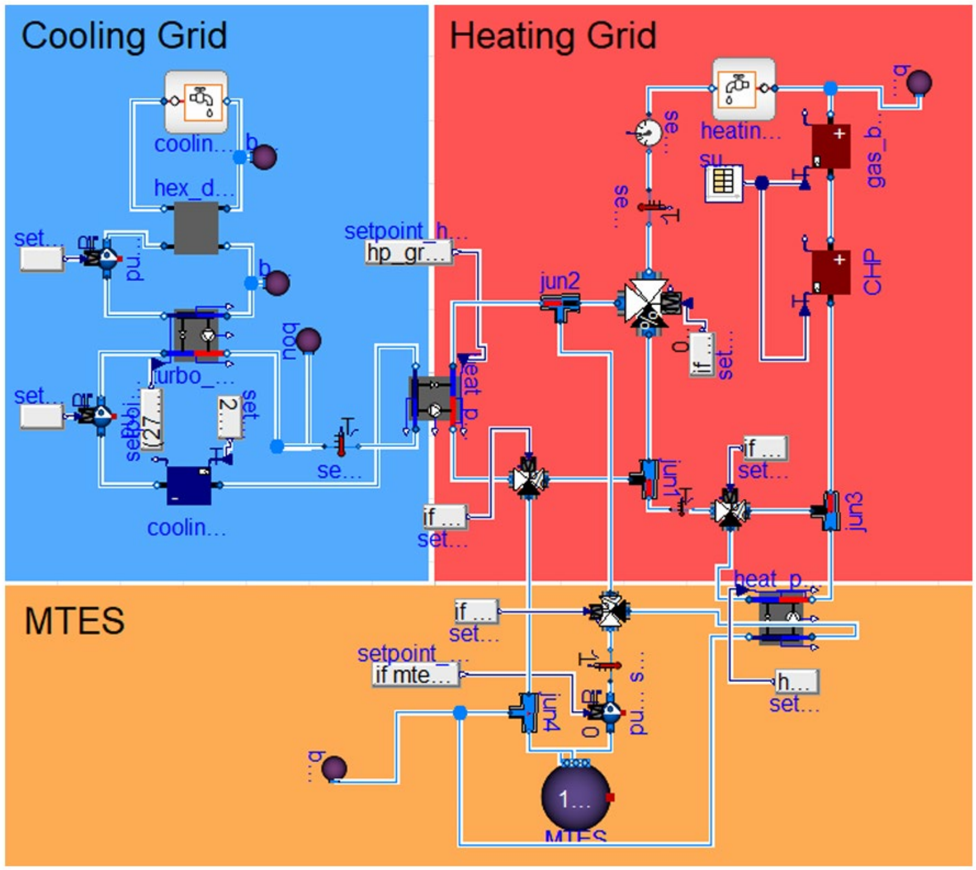

Figure 27: The new configuration of the heating and cooling system of the Ruhr-University Bochum in Modelica, showing the placement of the two heat pumps, the MTES, and the three-way valves relative to the CHP, gas boiler, turbo chillers, and cooling tower

The model is assembled from one-dimensional thermo-fluid components governed by mass, energy, and momentum balances, which together form a system of differential–algebraic equations. The CHP is an ideal heater tracking the heating demand up to 7.5 MW; it has priority over the heat pumps, and excess CHP heat cannot be stored, since the technical centre also supplies a neighbouring district. The gas boiler is likewise an ideal heater (forming a single unit with the CHP), and the cooling tower an ideal sensible-only cooler activating above its 22 °C target. The turbo chillers are a single block of total cooling capacity 10.8 MW (three units of 3.6 MW) with a Carnot efficiency of 0.4. Heat exchangers use a constant effectiveness of 0.76, and the heating and cooling demands are imposed as hourly time series with prescribed return temperatures, an internal controller setting the mass flow.

Two heat pumps are included: heat pump 1 transfers waste heat from the cooling cycle into the heating grid or the MTES, and heat pump 2 discharges the MTES into the heating grid. Both are the same size, defined by their condenser output and set to 2.5 MW in the reference case; although one heat pump could perform both duties, two identical units keep the operational strategy simple and the simulation robust (the techno-economic analysis later reverts to a single equivalent unit). Each COP is computed during the simulation from the Carnot COP scaled by a Carnot efficiency of 0.5 and a part-load efficiency, with a minimum 10 K lift between evaporator and condenser. The condenser setpoint depends on mode: zero when off, the heating supply temperature less the CHP minimum difference of 12.69 K when supplying the grid, and the 50 °C maximum MTES temperature when charging. Pump mass flow rates were taken from the existing installation, and pump electrical consumption was treated as negligible for the COP, since no pressure or head model was included.

Within the Modelica model the MTES itself is represented only by a coupling interface — a connection point for temperature and heat-flow exchange — because the storage physics reside in the Python model. The control strategy is implemented within the Modelica model as a set of if-statements that select among four operating scenarios and set the positions of the three-way valves and the component setpoints accordingly. The strategy acts only on the heating side, since the cooling side has a continuous waste-heat supply that is either used or rejected. The four scenarios are: a base case in which the heating demand is met by the CHP (with both heat pumps off, including the safety case in which a heat pump is disabled to prevent the predicted evaporator outlet temperature from falling below zero); MTES charging, in which surplus waste heat upgraded by heat pump 1 is stored while the demand is covered by the CHP and the storage remains below its maximum temperature; waste heat to the heating grid, in which heat pump 1 together with the CHP meets the remaining demand; and MTES discharge, in which heat pump 2 draws on the storage once heat pump 1 is at full capacity, subject to a sufficient temperature lift and the storage remaining above its minimum temperature. To keep the strategy robust, heat pump 1 cannot simultaneously charge the storage and supply the grid, and waste-heat supply to the grid is prioritised over charging.

The two models were coupled by exporting the Modelica model as an FMU and embedding it, together with the Python MTES model, within a single Python orchestration layer. The orchestrator coordinates the two participants using a non-iterative Gauss-Seidel master algorithm: at each communication step the storage model advances first, its output becomes the input to the Modelica model, which then advances over the same interval, after which the cycle repeats. Because the algorithm is non-iterative, each participant is advanced only once per communication step; the resulting extrapolation and interpolation errors, together with the local truncation errors of the explicit forward Euler scheme in Python and the adaptive C-language Variable-coefficients Ordinary Differential Equation (CVODE) solver in Dymola, accumulate as a function of the macro-step size and were accepted as a known characteristic of the coupling.

5.5. Simulation results

5.5.1. Base implementation

In the reference case study, the storage water temperature rises during summer and falls during winter, confirming that the system behaves as a seasonal storage. Short-term excursions trace back to the demand profile, which is shaped not only by space heating and cooling but also by activities such as laboratory experiments. The rock temperature follows the water temperature with a lag, rising while the water is warmer and falling when it is cooler, consistent with the conductive exchange built into the model (Figure 28).

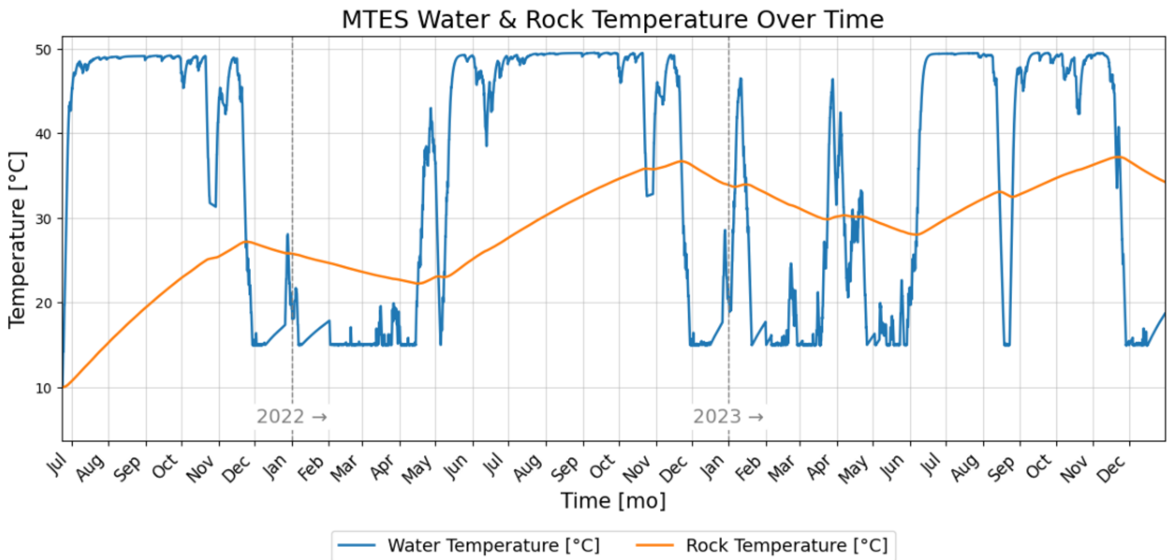

Figure 28: MTES water and rock temperature over the case-study simulation period [15]

The COP of the storage subsystem alone varies between zero and approximately 5.4. The total COP is 3.47, with a total output of 34.74 GWh and an input of 10.00 GWh. Zero values arise whenever the CHP alone meets the demand and no heat is transferred to the heating grid. These cluster in the warmer months, while the COP is high in winter, when the high heating demand allows extensive use of the storage system. Rapid COP fluctuations were traced back to the control strategy: heat pump 2 discharges the store, the storage temperature drops below the minimum level, the heat pump switches off, and the store recharges via conduction from the rock. This produces a characteristic on/off pattern.

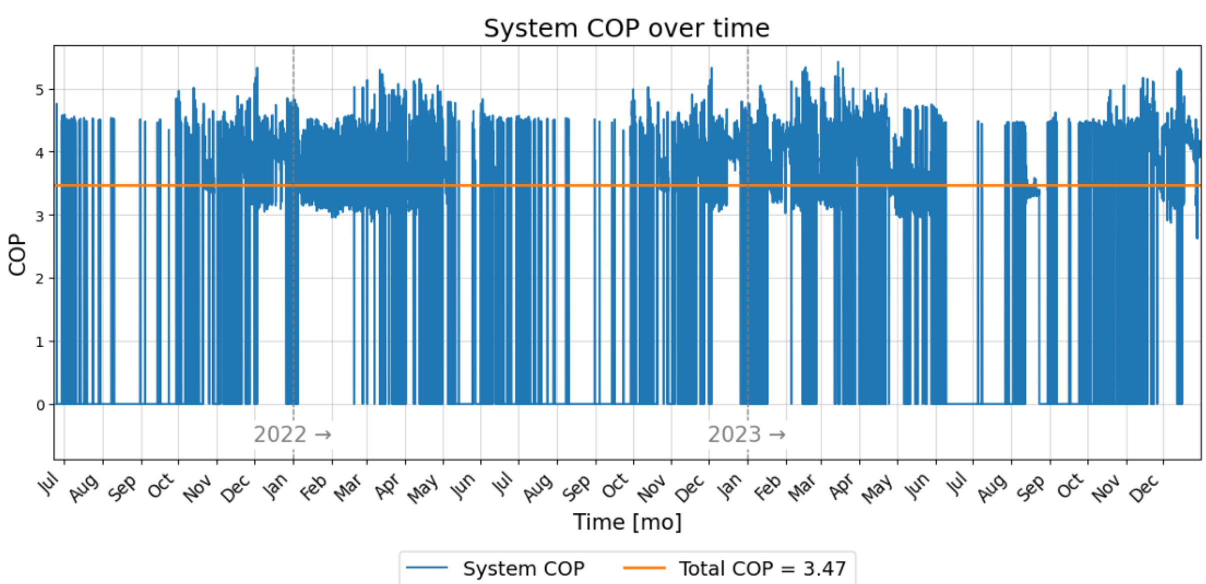

Figure 29: System COP over time (base case) shown together with the total COP [15]

5.5.2. Favourable implementation

The optimal practical setup applies the best parameters realisable within the existing site — a 5.5 MW heat pump, a ΔT of 5 K, the maximum feasible store volume of 10,000 m³, and a 50 °C maximum temperature. Relative to the case study it improves the technical metrics substantially: the total energy saved rises from 59.69 to 88.34 GWh, with the gas boiler and cooling tower reduced further still. The total COP falls to 2.49, but this reflects the larger and more heavily used heat pump rather than a loss of useful output, as discussed in Section 5.6. The longer-term behaviour supports this configuration: a 20.5-year run (looping the available data) shows the water temperature repeating its annual cycle while the rock charges over the first three years before settling into an oscillation between roughly 30 and 40 °C, so the store can be considered fully charged after about three years — a point worth noting, since the case study (only two-and-a-half years) had not yet reached this equilibrium.

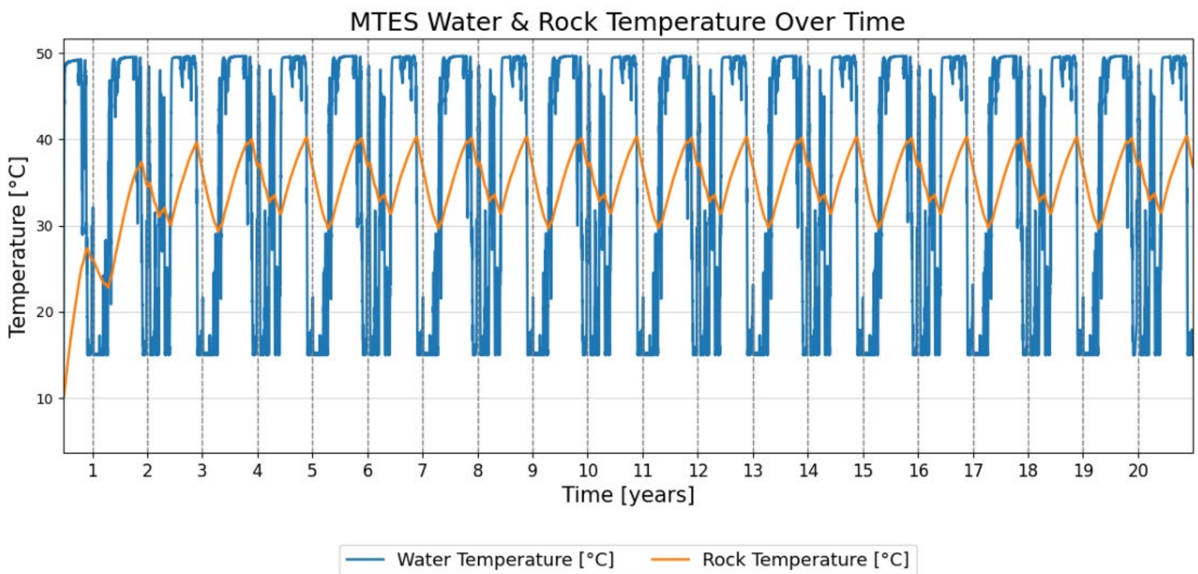

Figure 30: MTES water and rock temperature over the 20.5-year long-term simulation, showing the rock reaching thermal equilibrium after approximately three years [15]

5.5.3. Upscaled implementation

The optimal theoretical setup retains the same operating parameters but sizes the storage to the theoretical optimum for the available summer waste heat, corresponding to a volume of approximately 497,809 m³, which is far beyond the existing mine and therefore representing an upscaling case rather than a realisable design. This configuration improves the technical metrics further: the total energy saved rises to 119.94 GWh, and the water temperature rises almost continuously over the first one-and-a-half years, with the rock temperature climbing steadily as the larger rock volume adds thermal inertia. In both the favourable and upscaled configurations the gas boiler and cooling tower are substantially reduced and the heat pumps come to dominate the supply (Table 3), illustrating the upper bound of the technical potential of the Bochum MTES.

Table 3: Technical results of the base, favourable and upscaled implementations [15]

Variable	Base	Favourable	Upscaled
Heat-pump size [MW]	2.5	5.5	5.5
MTES volume [m³]	7,000	10,000	≈ 497,809
Total output [GWh]	34.74	52.83	63.34
Total input [GWh]	10.00	21.23	30.38
Total COP [-]	3.47	2.49	2.08
Gas-boiler energy saved [GWh]	34.74	52.83	63.34
Cooling-tower energy saved [GWh]	24.95	35.51	56.60
Total energy saved [GWh]	59.69	88.34	119.94

5.6. Discussion

The co-simulation results for the Bochum site demonstrate the clear technical feasibility of integrating Mine Thermal Energy Storage (MTES) into an existing district heating and cooling system. The MTES acts as an efficient thermal link between the waste-heat form the cooling side and the heating demand of the RUB. Moreover, as a seasonal buffer, the MTES successfully bridges the temporal mismatch between continuous waste heat generation from the cooling cycle and the peak winter demands of the heating cycle.

A central point of discussion arising from the simulation scenarios is the apparent paradox between the system's Coefficient of Performance (COP) and the total energy saved. In the base case, the system achieves a total COP of 3.47 while saving 59.69 GWh of energy. However, in the optimal practical setup (favourable implementation) utilizing a larger 5.5 MW heat pump and a 10,000 m³ storage volume, the COP decreases to 2.49, even though the total energy saved significantly increases to 88.34 GWh. This trend continues in the upscaled theoretical scenario, where the COP drops further to 2.08, but energy savings peak at 119.94 GWh.

This inverse relationship occurs because the larger heat pump is utilized more intensively and processes a substantially higher volume of lower-grade waste heat. While this requires a higher total electrical input—thus lowering the average COP—it effectively displaces a much larger share of the gas-boiler and cooling-tower operation. Consequently, maximizing the COP does not align with maximizing fossil fuel displacement; the absolute reduction in primary energy use is a far more vital metric for the system's overall decarbonisation impact.

Furthermore, the comparison between the practical and upscaled implementations highlights a fundamental geological limitation of the site. The theoretical volume required to capture all available summer waste heat is nearly 500,000 m³, which vastly exceeds the 10,000 m³ capacity of the existing accessible mine galleries. While the practical setup still yields substantial energy savings, the existing mine geometry acts as a physical bottleneck, meaning a portion of the available waste heat must still be rejected via the cooling towers.

Finally, the deliberate choice to use a low-order, physics-based Python model for the underground domain, rather than a highly resolved 3D numerical model, proved to be a good compromise between accuracy and computational expense. Also, given the high degree of uncertainty regarding the abandoned mine's precise geometry and thermal parameters, a 3D model would have introduced a false sense of precision. The reduced-order energy-balance approach successfully captured the essential seasonal thermal dynamics and phase-shifting necessary to evaluate the surface-side energy system, validating this pragmatic modelling choice.

5.7. Lessons learnt

- Thermal inertia dictates long-term evaluation horizons: The 20.5-year simulation run revealed that the rock surrounding the mine galleries requires approximately three years of charging and discharging cycles to reach a quasi-steady thermal equilibrium. Future MTES projects cannot be accurately evaluated based on their first year of operation; performance guarantees calculations must account for this multi-year transient start-up phase.
- Robustness of flexible co-simulation architectures: Embedding a Modelica-based surface network model as a Functional Mock-up Unit (FMU) directly within a Python orchestration layer proved to be a highly resilient approach. It effectively bridged the gap between equation-based surface dynamics and procedural subsurface balances, allowing both domains to be evaluated interactively without the need for cumbersome middleware.
- Strategic component sizing requires integrated testing: Evaluating the heat pumps and the MTES volume in isolation is insufficient. The sensitivity analysis demonstrated that the interaction between the extraction rate (heat pump size) and the buffer capacity (MTES volume) dictates the system's operational boundaries. Integrated co-simulation is essential to prevent oversizing surface components relative to geological limitations.

6. Conclusion

Co-Simulation has been applied to three PUSH-IT demonstration sites and three storage technologies: BTES in Darmstadt, ATES in Delft, and MTES in Bochum. In each case a domain-specific subsurface model was coupled to a surface-side energy system model with boundary conditions exchanged at defined synchronization points. The central, consistent finding is that this coupling captures behaviour neither domain reproduces alone: the feedback between the evolving subsurface temperature field and the surface-side operational decisions governs long-term performance and cannot be fully represented by standalone simulations.

General co-simulation framework and the different technical coupling approaches

Two coupling mechanisms were used successfully, direct Python APIs (FEFLOW via IFM, OpenDARTS, and the Python MTES model) and the FMI standard (Modelica models exported as FMUs into a Python orchestration layer) with the choice driven by the tools involved rather than any inherent advantage. The two represent different points on the balance between transparency and generality. Direct Python coupling retains the entire coupling logic, control strategy and data exchange within a single orchestration script, thereby avoiding file-based exchange or intermediate middleware. At Bochum, where the storage model is Python itself, the coupling is reduced to direct function calls within a single environment, providing maximum transparency and computational efficiency. However, it depends on the subsurface tool exposing a usable native interface. By contrast, FMI is tool-independent. A model exported as a self-contained FMU can be advanced step-by-step from the co-simulation master, independent of its environment. This is what enabled the detailed Modelica surface models to be integrated with the Python coupling infrastructure in a standardised way. The coupling error, however, resulting from a non-iterative master algorithm remains. Extrapolation and interpolation errors at communication steps, together with the solver's local errors, accumulate as a function of the macro-step size and must be managed by choosing the correct step size. Therefore, the choice between the two was governed by the available tools at each site rather than any inherent advantage. The direct route was simpler and more transparent where a subsurface simulator offered a clean Python API, whereas FMI provided the standardised bridge in cases where a Modelica model was required.

Results for the Darmstadt, Delft, and Bochum demonstration sites

The co-simulation produced two kinds of insight across the three sites. First, it revealed how each storage system behaves over its natural timescale. Second, it showed which design and integration choices determine whether a storage system becomes useful. Both insights are relevant to the design of future systems.

A first common finding concerns time. The early years of operation are not representative of long term behaviour, because each storage passes through a multi-year warming phase before it settles into a repeating annual cycle. The ATES wells at Delft stabilise over roughly six years, the rock at Bochum after about three, and the Darmstadt BTES field continues building its recoverable temperature over successive seasons. The practical consequence is that performance guarantees, recovery efficiencies, and cost estimates must therefore be based on multi-year horizons.

The decisive lesson at Darmstadt is that it is the hydraulic connection point, rather than the storage concept, which determines whether the BTES can be discharged. Connecting the storage downstream of a single building substation left the return flow too warm for heat extraction. However, relocating it to an aggregated central return pipe increased the fifth-year recovery efficiency from below 1.1 per cent to 20.9 per cent. Furthermore, increasing the number of boreholes from three to 37 raised the efficiency to 74.8 per cent. Therefore, the integration point and field size should be treated as primary design decisions.

Meanwhile, at Delft, the key takeaway is that storage performance is governed by the balance between geothermal supply, storage capacity and heat demand. A dynamic cutoff that permits discharge only when the hot well is warm enough relative to the network return shifted more of the supply to stored heat as the aquifer warmed. The upscaling scenarios showed that, in a supply-rich case, demand limits storage use, while, in a demand-rich case, surplus heat limits it. Therefore, the performance of an HT ATES system is strongly dependent on the relation between supply and demand, as well as the sizing and limits of the heat pump.

The central lesson in Bochum is that the objective at system level is more important than the efficiency of any single component. While a larger, more heavily used heat pump lowered the coefficient of performance, it displaced substantially more fossil fuel. Therefore, the absolute reduction in primary energy use is a more meaningful design target. The same effect was observed in Delft, confirming that storage should be evaluated based on its impact on the entire system rather than storage-specific metrics alone.

Transferable lessons learned regarding co-simulation methodology, model coupling strategies, and system behaviour that can inform future projects and upscaling efforts

Beyond the individual sites, the work provides insight into when to use which level of model detail. In an early design phase, when knowledge of the subsurface is limited, low-order models are the sensible choice. These models can be run quickly and allow for broad parameter studies and upscaling scenarios. As a project matures and the subsurface becomes better characterised, co-simulation with high-fidelity subsurface models becomes worthwhile because they reproduce the physically correct thermal and hydraulic behaviour, as well as the feedback between the storage system and the surface system, which lower-order models cannot capture. Another transferable result is that the same coupling framework worked across all three storage technologies and both coupling routes. This supports co-simulation as a general, reusable method rather than a site-specific solution.

Outlook

The models and coupling infrastructure developed in this task are carried forward within the project, most directly into the smart district heating controller development of Task 3.2. There, the co-simulation environment serves as the virtual demonstrator. The controllers are developed and tested against the coupled system models, which supply virtual measurements and receive control signals in place of the real installations. The co-simulation models further support the identification of the reduced-order models used within the controllers themselves, and remain available for scenario analysis of design variants, as illustrated by the Delft upscaling study in Section 5.5.5, which was performed with the Task 3.2 Modelica model of the site. The results of this deliverable thereby feed directly into the control implementation and virtual demonstration activities, extending the co-simulation framework from a performance assessment tool to the testing environment for the operational strategies to be deployed at the demonstration sites.

References

[1] J. Formhals, B. Welsch, H. Hemmatabady, D. O. Schulte, L. Seib, and I. Sass, “Co-simulation of district heating systems and borehole heat exchanger arrays using 3D finite element method subsurface models,” *Journal of Building Performance Simulation*, vol. 15, no. 3, pp. 362–378, May 2022, doi: 10.1080/19401493.2022.2058088.

[2] H.-J. G. Diersch, *FEFLOW: Finite Element Modeling of Flow, Mass and Heat Transport in Porous and Fractured Media*. Berlin, Heidelberg: Springer Berlin Heidelberg, 2014. doi: 10.1007/978-3-642-38739-5.

[3] D. Voskov *et al.*, “open Delft Advanced Research Terra Simulator(open-DARTS),” *JOSS*, vol. 9, no. 99, p. 6737, Jul. 2024, doi: 10.21105/joss.06737.

[4] Modelica Association, *Modelica® — A Unified Object-Oriented Language for Systems Modeling — Language Specification, Version 3.7*. 2026. [Online]. Available: https://specification.modelica.org/

[5] M. Wetter, W. Zuo, T. S. Nouidui, and X. Pang, “Modelica Buildings library,” *Journal of Building Performance Simulation*, vol. 7, no. 4, pp. 253–270, Jul. 2014, doi: 10.1080/19401493.2013.765506.

[6] B. Leitner, E. Widl, W. Gawlik, and R. Hofmann, “A method for technical assessment of power-to-heat use cases to couple local district heating and electrical distribution grids,” *Energy*, vol. 182, pp. 729–738, Sep. 2019, doi: 10.1016/j.energy.2019.06.016.

[7] F. Witte and I. Tuschy, “TESPy: Thermal Engineering Systems in Python,” *JOSS*, vol. 5, no. 49, p. 2178, May 2020, doi: 10.21105/joss.02178.

[8] T. Blockwitz *et al.*, “Functional Mockup Interface 2.0: The Standard for Tool independent Exchange of Simulation Models,” presented at the 9th International MODELICA Conference, Munich, Germany, Nov. 2012, pp. 173–184. doi: 10.3384/ecp12076173.

[9] M. Cacace and G. Blöcher, “MeshIt—a software for three dimensional volumetric meshing of complex faulted reservoirs,” *Environ Earth Sci*, vol. 74, no. 6, pp. 5191–5209, Sep. 2015, doi: 10.1007/s12665-015-4537-x.

[10] P. J. Vardon *et al.*, “A Research And Energy Production Geothermal Project On The TU Delft Campus: Project Implementation And Initial Data Collection,” in *PROCEEDINGS, 49th Workshop on Geothermal Reservoir Engineering*, Stanford University, 2024. [Online]. Available: https://geothermal.stanford.edu/events/workshop, https://pangea.stanford.edu/ERE/db/IGAstandard/search_results.php?showmax=99\&CONFERENCE=Stanford\%20Geothermal\%20Workshop\&SortField=Last1\&SortOrder=Ascend\&Find=Start\%20Search\&Year=2024

[11] T. Akın and A. Daniilidis, “Predictive Modeling of Heat Storage in TU DELFT Campus,” [Online]. Available: https://api.semanticscholar.org/CorpusID:276622117

[12] E. Kükrer, T. Akın, M. Bloemendal, A. Daniilidis, and P. J. Vardon, “Lessons learnt from integrating building demand and geothermal thermal energy storage systems,” in *Proceedings, Europen Geothermal Congress 2025*, Zürich, 2025.

[13] M. Bloemendal *et al.*, “High-Temperature Aquifer Thermal Energy Storage (HT-ATES) system for research development and demonstration on the TU Delft campus,” in *Proceedings, Europen Geothermal Congress 2025*, Zürich, 2025.

[14] D. V. Voskov, “Operator-based linearization approach for modeling of multiphase multi-component flow in porous media,” *Journal of Computational Physics*, vol. 337, pp. 275–288, May 2017, doi: 10.1016/j.jcp.2017.02.041.

[15] T. Spengler, “Co-Simulation of a District Heating and Cooling System in Combination with Mine Thermal Energy Storage.” Delft University of Technology, Delft, 2025. [Online]. Available: https://resolver.tudelft.nl/uuid:fddf8633-cca5-4b4e-b0ea-1a148c5d7340

The EU aims to have a net-zero greenhouse gas (GHG) economy by 2050, with 55% reduction on 1990 levels by 2030. At present, heating and cooling represent around 50% of the final energy demand in Europe and are mainly supplied by fossil fuel derived energy. It is therefore essential for heating and cooling to decarbonise to achieve EU ambitions.

A challenge for decarbonizing heat systems is the size of the seasonal mismatch between demand for heat and heat generation from sustainable sources – this mismatch is much larger than the equivalent intermittency in electricity supply and demand. The two main solutions to address this mismatch are: (i) to install a large capacity, so that peak demands can be met even at low production levels; or (ii) to store energy for later use if it is not needed at time of conversion. Many sustainable heat supply systems are characterised by high capital expenditure and low operational costs. Therefore, an installed capacity tailored at peak demand is not cost effective, while extending the annual operation period is advantageous for meeting energy needs, reducing levelised cost of energy (LCOE) and decarbonisation. Optimal utilisation of sustainable heat requires storing large amounts of heat to account for seasonal supply and demand fluctuations. Various technologies have been proposed for large-scale heat storage in geothermal reservoirs and low temperature storage is routinely applied. PUSH-IT focuses on extending storage temperature ranges to high temperatures. We will tackle remaining barriers, demonstrate applicability, increase public engagement, and optimise and de-risk operations. We will showcase three technology options that are fit for a wide variety of geological conditions covering most locations in Europe.

PUSH IT

Funded by the European Union